Genes and Environment, Vol. 31, No. 3 pp. 69-79 (2009)

Regular article

Development of Tester Strains Deficient in Nth/Nei DNA Glycosylases to Selectively Detect the Mutagenicity of Oxidized DNA Pyrimidines

Masami Yamada, Keiko Matsui, Atsushi Katafuchi, Makiko Takamune and Takehiko Nohmi[1]

Division of Genetics and Mutagenesis, National Institute of Health Sciences, Tokyo, Japan

(Received April 22, 2009; Revised May 30, 2009; Accepted June 9, 2009)

Oxidative DNA damage is a major cause of mutation and cell death in aerobic organisms. In addition to 8-hydroxyguanine, oxidized DNA pyrimidines play important roles in mutagenesis. Salmonella typhimurium TA1535, widely used in mutagenicity assays, carries a hisG46 missense mutation and efficiently detects mutations at G:C base pairs. To detect oxidative mutagens that selectively modify pyrimidines, we constructed a derivative of strain TA1535, termed YG3206, which lacks the Nei and Nth DNA glycosylases that excise oxidized pyrimidines from DNA. This novel strain easily detected the mutagenicity of L-cysteine, L-penicillamine, dopamine-HCl, and phenazine methosulfate, which are non-mutagenic or only weakly mutagenic in the TA1535 parent strain. A second strain that is equivalent to YG3206 but harbors the plasmid pKM101 which carries mucAB encoding DNA polymerase R1, termed YG3216, was significantly sensitive to phenazine ethosulfate. The compound was not mutagenic in either YG3206 or the Fapy-glycosylase-defective strain YG3001. Potassium bromate and methylene blue plus visible light with metabolic activation induced mutations in YG3001 but not YG3206 or YG3216. The number of spontaneous His$^+$ revertants per plate was 82 ± 16 (YG3206, ΔnthΔnei), 19 ± 4 (YG3001, Δfpg), and 6 ± 2 (TA1535), suggesting a significant contribution to spontaneous mutagenesis by endogenous pyrimidine oxidation. In the absence of exogenous chemical treatment, exposure to fluorescent light enhanced the spontaneous mutation frequency by approximately two-fold (YG3206), 13-fold (YG3001), and 10-fold (TA1535). These results suggest that certain environmental chemicals may selectively introduce mutagenic damage at DNA pyrimidines, and that these changes can be monitored by the use of YG3206.

Key words: genotoxicity, oxidative damage, oxidized pyrimidines, Endo III, Endo VIII

Introduction

The DNA of all organisms is constantly damaged by endogenous processes, including oxidation, hydrolysis, and alkylation (1,2). A potential source of the large number of mutations produced during tumor progression is DNA damage, particularly damage by reactive oxygen species (ROS) (3). In aerobically grown cells, ROS are produced as by-products of normal metabolic pathways and have been shown to contribute to human diseases, including cancer, cardiovascular disease, immune system decline, and brain dysfunction (4). Some of the byproducts include singlet oxygen ($^1O_2$), peroxide radicals ($^{\cdot}O_2$), hydrogen peroxide (H_2O_2), and hydroxyl radicals ($^{\cdot}OH$) (5). The reactions mediated by ROS can lead to a wide variety of DNA damage, including DNA strand breaks, protein-DNA cross-links, abasic sites, and base lesions (6). Although cells possess many defenses against oxidative damage, it has been estimated that the mammalian genome undergoes roughly 10^4–10^5 oxidative attacks per day (4).

More than 50 different base lesions have been identified as the products of oxidative DNA damage (7). Arguably, the DNA base lesion receiving the most attention is 8-hydroxy-2′-deoxyguanosine (8-OH-dG, 7,8-dihydro-8-oxo-2′-deoxyguanosine), which is commonly used as a biomarker of oxidative DNA damage in the cell (8,9). When 8-OH-dG is present in a DNA template, A or C is inserted opposite 8-OH-dG, depending on the specific polymerase involved (10–12). In bacterial and mammalian cells, 8-OH-dG has been shown to produce high levels of G:C to T:A transversion mutations (13). In *Escherichia coli*, some enzymes are involved in processing 8-OH-dG-induced oxidative DNA damage (14). One enzyme is MutM glycosylase, or formamide pyrimidine DNA glycosylase (FPG), which is encoded by *mutM* or *fpg* and removes 8-hydroxyguanine (8-OH-G, 7,8-dihydro-8-oxoguanine) lesions found in DNA (15,16).

Oxidized pyrimidines also contribute mutations. For

[1]Correspondence to: Takehiko Nohmi, Division of Genetics and Mutagenesis, National Institute of Health Sciences, 1-18-1, Kamiyoga, Setagaya-ku, Tokyo 158-8501, Japan. Tel: +81-3-3700-9872, Fax: +81-3-3700-2348, E-mail: nohmi@nihs.go.jp

instance, several studies have hinted at a significant contribution of oxidized uracil derivatives, such as 5-hydroxyuracil (5-OH-U) or uracil glycol (Ug), to G:C to A:T transitions in *E. coli*. An initial oxidation of cytosine is followed by deamination to a poorly repaired uracil derivative, which is one of the most frequent forms of endogenous DNA damage and strongly miscoded during replication (17). The hydrolytic deamination of 5-methyl cytosine (5mC) to thymine generates a thymine mispaired with guanine (18). Mutations resulting from 5mC comprise one of the most frequent classes of point mutation found in human cancer cells (19). The damaged pyrimidines are generally removed by glycosylases that cleave the bond between the sugar and N1 position of the damaged base (20). In the human genome, several different glycosylases with uracil-DNA glycosylase activity have been identified, and many of these share substantial homology with uracil DNA glycosylases found in other organisms (20).

In *E. coli*, Nth glycosylase, or endonuclease III (Endo III), and Nei glycosylase, or endonuclease VIII (Endo VIII), are base excision repair proteins with overlapping substrate specificities that remove oxidized pyrimidine bases from DNA (21,22). Upon the recognition of an oxidized pyrimidine by a DNA glycosylase, the *N*-glycosylic bond is cleaved, releasing the free base. This event is followed by the cleavage of the phosphodiester backbone by an associated DNA lyase activity, which leaves a blocked 3′ terminus in the resulting nick (23). The block, either an α,β-unsaturated aldehyde or a phosphate, must be removed by the phosphodiesterase or phosphatase activity of another class of enzymes, the 5′ AP endonucleases. This phenomenon results in a single base gap, which is filled in by DNA polymerase and sealed by DNA ligase (24). Endo III and Endo VIII remove potentially lethal lesions, such as thymine glycol and urea, that are blocks to DNA synthesis *in vitro* and lethal *in vivo* (25,26). Endo III and VIII also remove free radical damaged cytosines, Ug, dihydrouracil, 5-OH-U, and 5-hydroxycytosine, all of which are mutagenic (17,27) and can mispair with adenosine during DNA synthesis *in vitro* (28).

We previously reported that *Salmonella typhimurium* strains YG3001, YG3002, and YG3003 are highly sensitive to oxidative mutagens due to a lack of $mutM_{ST}$ encoding FPG (29). The strains are derivatives of Ames tester strains TA1535, TA1975, and TA102, respectively, which are widely used for the identification of environmental mutagens and carcinogens. In this study, we disrupted the genes encoding Endo III and Endo VIII in *S. typhimurium* TA1535, i.e., nth_{ST} and nei_{ST}, respectively, to establish strain YG3206. To evaluate chemical sensitivity, we selected well-known oxidative agents and those reported to be mutagenic in the tester strains sensitive to oxidative mutagens (30,31). The references therein also suggested some chemicals to be screened. Because strains YG3206 and YG3001 lack Nth/Nei and FPG, respectively, we expected that a comparison of sensitivities would identify chemicals that preferably oxidize pyrimidines or purines in DNA. Our results suggest that L-cysteine and four other chemicals may predominantly oxidize pyrimidines in DNA, thereby inducing mutations. In contrast, potassium bromate and three other chemicals seem mainly to oxidize purines in DNA. Collectively, the results suggest that the chemicals induce oxidative mutagenesis through different mechanisms, and that newly established strains YG3206 and YG3216 are useful for identifying chemicals that induce mutations through the oxidation of pyrimidine in DNA.

Materials and Methods

Strains and plasmids: The strains and plasmids used in this study are listed in Table 1.

Oligonucleotides: Oligonucleotides used for PCR amplification were purchased from Japan Bioservice (Ibaraki, Japan). Each sequence is shown in the text. The one including a thymine glycol used for DNA glycosylase assay was commercially obtained from Tsukuba Oligo Service Co., Ltd. (Tsukuba, Japan), where the oligonucleotide was applied on a poly acrylamide gel, then the corresponding band was purified from the gel after running.

Media: Luria-Bertani broth and agar were used for bacterial culture. Vogel-Bonner minimal agar plates and top agar were prepared as previously described (32) and used for the His^+ reversion assay with *S. typhimurium*. Nutrient broth (Difco, MI, U.S.A.) was used in the precultures for the reversion assay. Ampicillin (Ap, 50 μg/mL), kanamycin (Km, 25 μg/mL), or chloramphenicol (Cm, 10 μg/mL) were supplemented in overnight cultures for strains harboring pKM101, $\Delta mutM$::*kan*, or Δnei_{ST}::*cat*, respectively. Liver S9 prepared from male Sprague-Dawley rats pretreated with phenobarbital and 5,6-benzoflavone was purchased from Kikkoman Cooperation (Chiba, Japan).

Construction of the Endo III-deficient strain: We introduced a stop codon, TGA, in the coding region of nth_{ST} in TA1535 without any drug-resistance marker (33). The nth_{ST} gene and its flanking region were amplified by PCR using the chromosome DNA of TA1535 and the primers 5′-CAC AAC GCT GGT ATT AAC GCT GAC-3′ and 5′-GCA CTG AAG GAA GAG AAA AGG GTG-3′, and then cloned into an *Aat*II site of the pBR322 vector. The resultant plasmid, pYG433, was digested with *Sca*I and *Eco*RV, and the resulting 2-kb fragment was sub-cloned into *Sma*I site of the pKO3 vector (Table 1). The pKO3 vector has *cat* and *sacB*, used for selection as described below. The resultant plasmid, pYG437, included nth_{ST} and was

Table 1. List of the strains and plasmids used in this study

	Genetic characteristics	Source
Strain		
TA1535	*hisG46, gal,* Δ(*chl, uvrB bio*) *rfa*	(32)
YG3001	The same as TA1535, but deficient in $mutM_{ST}$, Km^R	(29)
YG3201	The same as TA1535, but deficient in nei_{ST}, Cm^R	This study
YG3203	The same as TA1535, but deficient in nth_{ST}	This study
YG3206	The same as TA1535, but deficient in nth_{ST} and nei_{ST}, Cm^R	This study
TA100	The same as TA1535, but harbors pKM101, Ap^R	(32)
YG3008	The same as TA3001, but harbors pKM101, Ap^R, Km^R	(29)
YG3216	The same as TA3206, but harbors pKM101, Ap^R, Cm^R	This study
Plasmid		
pYG432	derivative of pBR322, carrying nei_{ST} at the *Aat*II site, Tc^R	This study
pYG434	derivative of pBR322, carrying nei_{ST} disrupted with *cat*-replacement, Cm^R, Tc^R	This study
pYG433	derivative of pBR322, carrying nth_{ST} at the *Aat*II site, Tc^R	This study
pYG437	derivative of pKO3, subcloning the *Sca*I-*Eco*RV fragment, including nth_{ST} from pYG433, into the *Sma*I site, Cm^R	This study
pYG438	derivative of pKO3, carrying nth_{ST} which has a four-base deletion, Cm^R	This study
pBR322	vector plasmid, Ap^R, Tc^R	Laboratory stock
pKO3	vector plasmid with temperature-sensitive replication origin, Cm^R	(33)

Km^R, kanamycin resistant; Cm^R, chloramphenicol resistant; Ap^R, ampicillin resistant; Tc^R, tetracycline resistant.

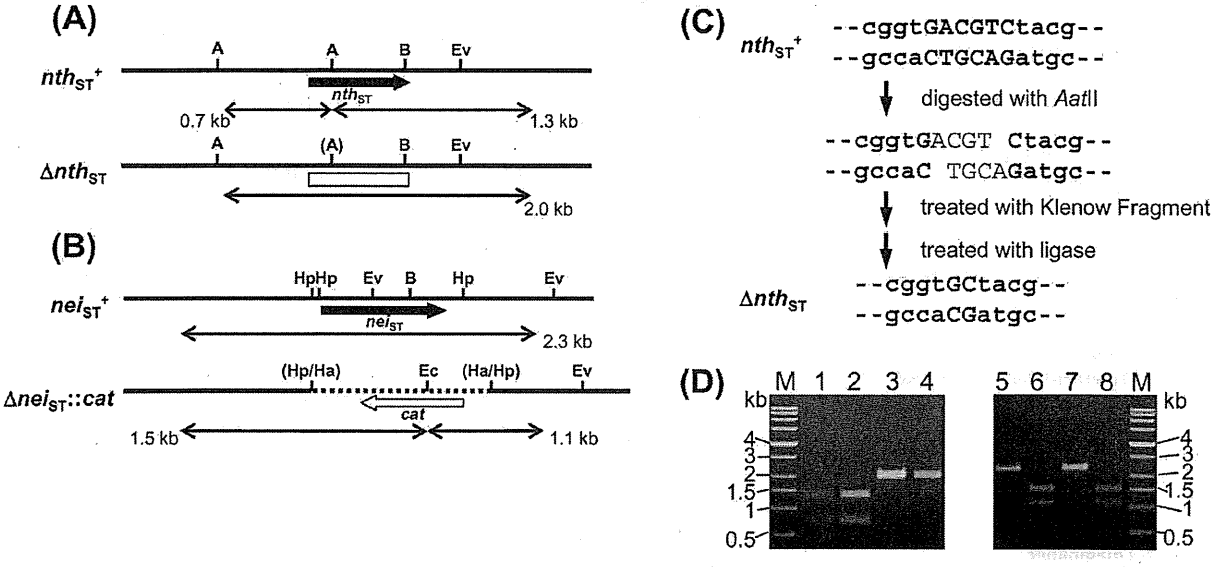

Fig. 1. Disruption of the nth_{ST} and nei_{ST} genes. Partial restriction maps of nth_{ST} (A) and nei_{ST} (B) and the surrounding chromosomal region in the original TA1535 strain and its deletion recombinants. Thick black arrows indicate the position and transcriptional direction of the genes in wild-type (A) and (B). The white box (A) exhibits a deficient nth_{ST} gene possessing the introduced frameshift mutation. The dotted line (B) indicates the replaced fragment, including the *cat* gene shown with a white arrow. The size of the bands amplified by PCR or digested with restriction enzymes after the PCR reaction is shown at each line in (A) and (B). Restriction enzyme sites are shown as follows: A, *Aat*II; (A), missing *Aat*II site; B, *Bgl*II; Ec, *Eco*RI; Ev, *Eco*RV; Ha, *Hae*II; Hp, *Hpa*I. (Hp/Ha) and (Ha/Hp) represent the junctions of the *Hae*II fragment when it was inserted into the *Hpa*I site in nei_{ST}. (C) The scheme shows how to produce the deletion/frameshift in nth_{ST} at the *Aat*II site, i.e., GACGTC. Four base pairs, ACGT, are deleted at the end of the procedure. (D) The pictures of the agarose gel exhibit the bands after restriction enzyme digestions. Left: *Aat*II digestion for Δnth_{ST} strain construction. Right: *Eco*RI digestion for Δnei_{ST} strain construction. M, size marker; lanes 1 and 5, TA1535; lanes 2 and 6, YG3201; lanes 3 and 7, YG3203; lanes 4 and 8, YG3206.

digested with *Aat*II (Takara Bio, Ootsu, Japan) (Fig. 1A). The cleaved plasmid was treated with Klenow fragment (New England Biolabs) to make both ends blunt (Fig. 1C). After ligation of the ends, four bases (ACGT) were deleted, which generated a TGA at the 46th codon of nth_{ST}. The obtained plasmid, pYG438, was introduced into TA1535, and Cm-resistant colonies were selected at 43°C to identify clones in which the plasmid was integrated into the chromosome. Then, the Cm-resistant colonies were examined to determine whether

they could survive on LB plates with 5% sucrose. Only clones in which the integrated *sacB*-containing fragment was removed were able to form colonies on the plates because the *sacB* gene product converts sucrose to a toxic substance. The lack of ACGT in nth_{ST} was verified by digestion of the PCR product with the *Aat*II restriction enzyme, followed by 0.8% agarose gel electrophoresis (Fig. 1D). The clones with PCR products tolerant to *Aat*II digestion were designated as YG3203, i.e., TA1535 Δnth_{ST}. The set of primers used for amplification were the same as for cloning.

Construction of the Endo VIII-deficient strain: The nei_{ST} gene and its flanking region, with a total size of 2.3 kb, was amplified by PCR using the chromosome DNA of TA1535 and primers 5′-GTA TTT GCT GGT TCT TTA GGT GCG C-3′ and 5′-GTG ATC TGG TTT CCG CCG CTT A-3′, and the amplified fragment was cloned into an *Aat*II site of the pBR322 vector. Using the resultant plasmid, pYG432 (Table 1), nei_{ST} was disrupted by the pre-ligation method (34). Briefly, pYG432 was digested with the *Hpa*I enzyme, and an approximate 1-kb region containing nei_{ST} was replaced with a *cat* gene cassette (Fig. 1B). The resultant plasmid, pYG434, was digested with *Apa*LI, and T4 DNA ligase joined both ends of the 5-kb fragment. The treated DNA was introduced into TA1535 and Cm-resistant

Table 2. List of the chemicals used in this study

	Chemical	CAS registry number	Molecular weight	Solvent	Source†
1	L-cysteine	52-90-4	121.15	H_2O	Wako
2	L-penicillamine	1113-41-3	149.21	H_2O	TCI
3	Dopamine-HCl	62-31-7	189.64	H_2O	Wako
4	Phenazine methosulfate (PMS)	3130-59-4	306.34	H_2O	Wako
5	Hydrogen peroxide (H_2O_2)	7722-84-1	34.01	H_2O	Wako
6	Phenazine ethosulfate (PES)	10510-77-7	334.39	H_2O	Dr. Ohta
7	Potassium bromate ($KBrO_3$)	7758-01-2	167.00	H_2O	Wako
8	Methylene blue (MB)*	61-73-4	319.86	H_2O	Sigma
9	Neutral red (NR)*	553-24-2	288.78	H_2O	Sigma
10	Benzo[*a*]pyrene (B[*a*]P)*	50-32-8	252.31	DMSO	Wako
11	2-Nitrofluorene	607-57-8	211.22	DMSO	TCI
12	Glyoxal	83513-30-8	58.04	H_2O	TCI
13	Kethoxal	27762-78-3	148.16	DMSO	Sigma
14	Methylglyoxal	78-98-8	72.06	H_2O	Sigma
15	*N*-Nitrosotaurocholic acid (*N*-NTCA)	82660-96-6	544.70	H_2O	Dr. Totsuka
16	Paraquat	2074-50-2	257.16	H_2O	Wako
17	Phenylhydrazine	100-63-0	108.14	DMSO	Wako
18	Hydroquinone	123-31-9	110.11	H_2O	Wako
19	2,6-Dimethyl-1,4-benzoquinone	527-61-7	136.15	DMSO(10 mg/mL)→W+	Wako
20	Duroquinone	527-17-3	166.22	DMSO(1 mg/mL)→W	Wako
21	Menadione	58-27-5	172.18	DMSO(1 mg/mL)→W	Wako
22	Lawsone (2-hydroxy-1,4-naphthoquinone)	83-72-7	174.15	DMSO(5 mg/mL)→W	TCI
23	Acetaldehyde	75-07-0	44.05	H_2O	Merck
24	Methoxsalen	298-81-7	216.19	DMSO	Sigma
25	Catechol	120-80-9	110.11	H_2O	TCI
26	2,5-Toluquinone	553-97-9	122.12	DMSO(20 mg/mL)→W	Wako
27	1,4-Benzoquinone	106-51-4	108.09	DMSO(10 mg/mL)→W	Wako
28	l-Dopa	59-92-7	197.19	0.5N NaOH(50 mg/mL)→W	TCI
29	Cumene hydroperoxide	80-15-9	152.2	DMSO(5 mg/mL)→W	Aldrich
30	*t*-Butyl hydroperoxide	75-91-2	90.12	H_2O	Wako
31	4-Oxo-2-hexenal	2492-43-5	112	DMSO	Dr. Kawai
32	Psolaren	66-97-7	186.16	DMSO	Sigma
33	Spermine NONOate	136587-13-8	262.4	0.1N NaOH(5 mg/mL)→W	Sigma
34	*S*-nitroso-*N*-acetyl-dl-penicillamine	79032-48-7	220.25	DMSO	Sigma
35	1,3-Butadiene diepoxide	1464-53-5	86.09	DMSO	Wako
36	Formaldehyde	50-00-0	30.03	H_2O	Wako
37	Glutaraldehyde	111-30-8	100.12	H_2O	Wako
38	Plumbagin	481-42-5	188.18	DMSO	TCI
39	Bleomycin hydrochloride	67763-87-5	1453.02	H_2O	Wako
40	Thiabendazole	148-79-8	201.3	DMSO	Wako

*: These chemicals were used for visible light irradiation assay.
†: Wako, Wako Pure Chemicals; Sigma or Aldrich, Sigma-Aldrich Chemicals; TCI, Tokyo Chemical Industry.
+: "→W" means that the chemical was initially dissolved in DMSO or NaOH solution, then diluted with water according to its solubility.

colonies were selected. The *Eco*RI site is present only in *cat* and not in nei_{ST} (Fig. 1B). The replacement of nei_{ST} with *cat* was confirmed by PCR amplification using the cloning primers, followed by digestion with *Eco*RI (Fig. 1D). The resultant strain, TA1535 with Δnei_{ST}::*cat*, was designated as YG3201. In the same way, YG3206, i.e., TA1535$\Delta nth_{ST}\Delta nei_{ST}$::*cat*, was constructed using YG3203 instead of TA1535 (Fig. 1D). Introducing pKM101 into YG3206 resulted in YG3216, i.e., TA1535$\Delta nth_{ST}\Delta nei_{ST}$::*cat*/pKM101 (Table 1).

DNA cleavage assay: Crude lysate was prepared from a 40-mL culture at an OD_{600} of 0.6–0.7 as previously described (35). One picomole of each Cy3-labeled duplex oligonucleotide (5′-Cy3-CTC GTC AGC ATC T TgC ATC ATA CAG TCA GTG-3′ and 3′-GAG CAG TCG TAG AAG TAG TAT GTC AGT CAC-5′, Tg is thymine glycol) were incubated at 37°C for 30 min with various amounts of the crude lysate derived from TA1535, YG3201, YG3203, or YG3206 in 10 μL reaction mixtures containing 10 mM Tris-HCl (pH 7.5), 1 mM EDTA, 100 mM NaCl, and 0.1 mg/mL BSA. The crude lysate was diluted to include 1, 3, or 10 μg of protein in each reaction. Strain AB1157 of *E. coli* was used in the same way as a positive control of crude lysate because it has both glycosylase activities. After incubation, the reactions were terminated by the addition of loading buffer (98% formamide, 10 mM EDTA, 20 mg/mL blue dextran). The samples were then heated at 95°C for 5 min and immediately cooled on ice. The samples were loaded onto 15% polyacrylamide denaturing gels containing 8 M urea. After electrophoresis at 2000 V, the gels were scanned by the Molecular Imager FX Pro System (BioRad, USA) to detect Cy3 fluorescence. The intensity of each band was determined by Quantity One software (BioRad). As a control, purified Endo III (1 unit) and Endo VIII (10 units) (New England Biolabs, USA) were used.

Chemicals: The names, abbreviations, CAS registry numbers, molecular weight, solvent to dissolve the chemicals, and sources of the chemicals assayed in this study are listed in Table 2. Phenazine ethosulfate, *N*-nitrosotaurocholic acid, and 4-oxo-2-hexenal were kindly provided by Drs. Toshihiro Ohta from Tokyo University of Pharmacy and Life Sciences, Yukari Totsuka in National Cancer Center Research Institute, Tokyo, and Kazuaki Kawai in University of Occupational and Environmental Health Japan, Kitakyushu, respectively.

Mutagenicity assay: The mutagenicity assay was carried out with a pre-incubation procedure (32). Briefly, 0.1 mL of overnight culture was incubated with the chemicals dissolved in 0.1 mL of solvent and 0.5 mL of 1/15 M phosphate buffer (pH 7.4) for 20 min at 37°C. The S9 mix was added instead of the buffer for the assay using methylene blue (MB). The mixture was then poured onto agar plates with soft agar and incubated for 2 days at 37°C in the dark. Each chemical was assayed with 4–7 doses on triplicate plates with six strains, TA1535, YG3001, YG3206, TA100, YG3008, YG3216, in parallel.

White fluorescent light irradiation: Methylene blue, neutral red (NR), and benzo[*a*]pyrene (B[*a*]P) were subjected to the assay with plates that were irradiated with white fluorescent light, which was delivered by a fluorescent lamp (15W, 370–750 nm wavelength) during the 2-day incubation at 37°C. The plates were placed upside down 50 cm from the light source. The light intensity of 1,000 lx was measured with an Illumination meter (IM-1, Tokyo Kogaku Kikai K.K., Tokyo, Japan). Plates not exposed to light were covered with sheets of aluminum foil during the incubation. In addition, room lights were turned off during the experiments to distinguish between the results with- and without-irradiation conditions. Spontaneous mutagenicity in the irradiated-condition was also examined in this manner.

Results

Establishment of S. typhimurium strains deficient in Endo III and/or VIII: Our aim was to develop a system to identify chemicals that cause mutations via oxidized pyrimidines. The gene encoding Endo III (nth_{ST}^{+}) was disrupted by recombination and confirmed by PCR and restriction-enzyme digestion. *Aat*II digestion cleaved the 2-kb DNA fragment containing the nth_{ST} from the parental strain, TA1535, into two fragments 1.3 kb and 0.7 kb in size (Figs. 1A and D, Lane 1), whereas the fragment amplified with the same primers from the nth_{ST}-disrupted strain was not cleaved, which is consistent with the expected loss of the *Aat*II site in the disruptant (Figs. 1A, C and D, Lane 3). The nth_{ST}-disrupted strain was designated YG3203. A similar approach was used to inactivate nei_{ST} in TA1535 (Fig. 1B) to generate YG3201. *Eco*RI digestion did not cleave the fragment from the parental strain (Fig. 1D, Lane 5), whereas the same fragment from the nei_{ST}-disrupted strain was cleaved into two fragments 1.5 kb and 1.1 kb in size (Fig. 1D, Lane 6). This finding is consistent with the expected addition of the *Eco*RI site derived from the insertion of *cat* in the disruptant (Fig. 1B). The nth_{ST}/nei_{ST} double mutant, designated YG3206, was obtained by introducing nei_{ST}::*cat* into YG3203 (Fig. 1D, Lanes 4 and 8).

We examined whether the strains appropriately lost the endonuclease activities for the substrates (Fig. 2). The endonuclease activities were detected in the crude extracts of parental strain TA1535 and *E. coli* strain AB1157, which possesses counterparts to Endo III and VIII. The positions of nicked products I and II (35) formed by treatment with the crude extracts of TA1535 and AB1157 (Fig. 2, Lanes 4–6 and 16–18) were identi-

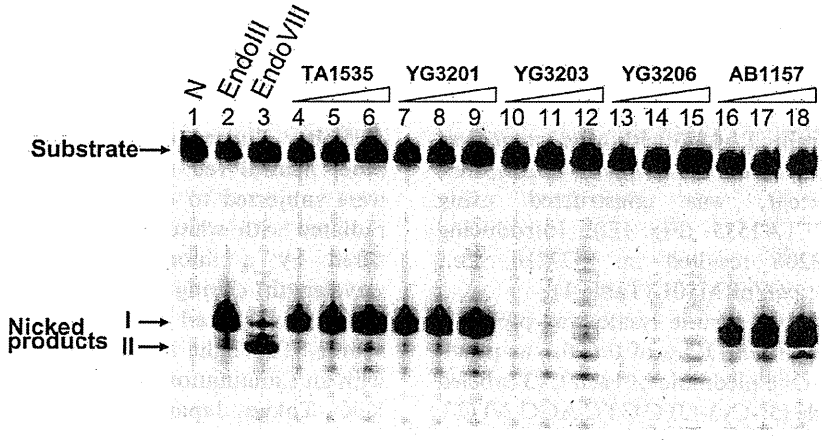

Fig. 2. PAGE analysis of the reaction products formed by the incubation of oligonucleotide substrates containing thymine glycol with Endo III and Endo VIII or crude lysates. The annealed oligonucleotides were incubated with different amounts of the indicated enzymes or crude lysates at 37°C for 30 min. Nicked products were separated by 15% denaturing PAGE. The image of the gel is shown. Lane 1, primer without reaction; lane 2, Endo III; lane 3, Endo VIII; lanes 4–6, TA1535; lanes 7–9, YG3201; lanes 10–12, YG3203; lanes 13–15, YG3206; lanes 16–18, AB1157. Three arrows indicate, in order starting from the top, the position of substrate, product I for Endo III activity, and product II for Endo VIII activity.

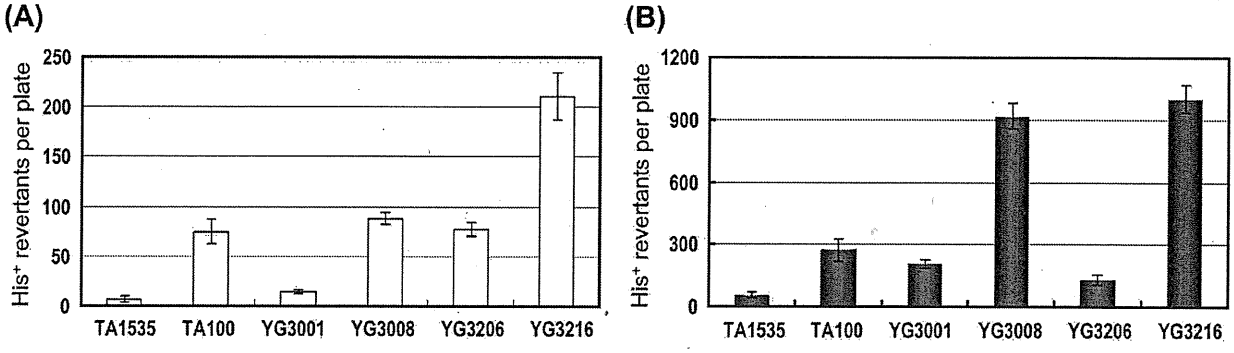

Fig. 3. Spontaneous mutagenicity in *S. typhimurium* strains deficient in DNA glycosylases. The assay was carried out in the dark (A) and under irradiation with a fluorescent light (B) as described in Materials and Methods. Strains are indicated at the bottom of the graphs. The height of bars represents the numbers of spontaneous His^+ revertants per plate and the standard deviations.

cal to the bands generated by the treatment of the substrate with purchased Endo III and VIII (Fig. 2, Lanes 2 and 3). Comparing nicked product I in the lanes for TA1535 and AB1157 with those of YG3203 and YG3206, it is clear that strains YG3203 and YG3206 lost Endo III activity (Fig. 2, Lanes 10–15). Comparing the bands at the position of nicked product II, YG3206 also lost Endo VIII activity (Fig. 2, Lanes 13–15). Thus, we conclude that YG3206 lost both Endo III and VIII activities.

Spontaneous mutagenesis: The number of spontaneous His^+ revertants per plate was examined in the newly constructed strain YG3206, $\Delta nth_{ST}\Delta nei_{ST}$, and five reference strains: the TA1535 parent strain, its $\Delta mutM_{ST}$ derivative, YG3001, and their respective pKM101-harboring strains, TA100 and YG3008. We also included YG3216, the pKM101-harboring version of YG3206. The plasmid pKM101 works for efficient bypasses of DNA lesions caused by chemicals. These results are summarized in Fig. 3. For YG3206, $\Delta nth_{ST}\Delta nei_{ST}$, there were 82 ± 16 revertants per plate; for YG3001 and TA1535, the values were 19 ± 4 and 6 ± 2, respectively (Fig. 3A). To further validate these strains, we determined the effect of fluorescent light on their spontaneous mutation frequencies. In the absence of any other exogenous DNA-damaging treatment, irradiation alone enhanced mutation by more than 10-fold in YG3001, roughly two-fold in YG3206, and 10-fold in TA1535 (Fig. 3B). Irrespective of irradiation, the pKM101-harboring strains produced more revertants than their respective non-pKM101 strains.

Specificity and sensitivity of YG3206: The mutagenicity of 40 chemicals (Table 2) was compared among the six strains mentioned above (Table 1). Two-thirds of the tested chemicals were not mutagenic in any of the strains and exhibited neither dose responses nor 2-fold

Table 3. Mutagenic sensitivity to the chemicals in *S. typhimurium* strains deficient in $mutM_{ST}$ or nei_{ST}/nth_{ST}

Chemicals	Group*	TA1535	YG3001	YG3206	Dose† (μg/plate)	TA100	YG3008	YG3216	Dose† (μg/plate)
		Induced His^+ revertants per μmol chemical				Induced His^+ revertants per μmol chemical			
L-cysteine	A	ND‡	ND	6.5	2500	11	17	130	500
L-penicillamine	A	ND	1.1	57	2000	8.3	12	170	1000
Dopamine-HCl	A	ND	ND	21§	500	ND	ND	230	100
PMS	A	ND	ND	3,400§	5	ND	ND	9,800§	5
H_2O_2	A	ND	ND	238,000	0.02	116,000§	252,000§	1,153,000§	0.01
PES	A′	ND	ND	ND		ND	ND	3,700	25
$KBrO_3$	B	ND	1.2	ND	2500	ND	ND	ND	
MB+S9+light	B	400	5,700	ND	25	7,200	14,000	ND	25
NR+light	B	8,200	51,000	19,000	1	22,000	51,000§	64,000§	1
B[*a*]P+light	B	1,600	8,900	1,300	10	14,000	39,000	11,000	10
2-Nitrofluorene	C	ND	ND	ND		36,000	23,000	66,000	5
Glyoxal	C	ND	ND	ND		510	510	1,000	50
Kethoxal	C	ND	ND	ND		24,000	2,900	7,400	10
Methylglyoxal	C	ND	ND	ND		13,000	800	2,500	10
N-NTCA	D	11,000	11,000	10,000	50	—‖	—	10,000	50

These results were confirmed at least three times. The numbers are the mean values of induced His^+ revertants per μmol chemical in triplicate plates or three independent assays with a single plate.
*: The definition is in the text.
†: Dose used for calculation of the numbers of induced His^+ revertants in the category.
+: ND: No mutagenicity was detected, which means no dose response and less than 2-fold increase in the number of induced His^+ revertants per plate.
§: These values were not 2-fold more than those for the solvent control, but the results indicated a clear dose-response in the number of induced His^+ revertants per plate.
‖: The dash indicates that the value was not examined.

increases in the number of His^+ revertants per plate (data not shown). The chemicals listed in Table 3 were mutagenic in some or all of the strains tested. Based on the order of strain sensitivity, we classified the chemicals into Groups A to D as follows.

Group A compounds: L-cysteine, L-penicillamine, dopamine-HCl, phenazine methosulfate (PMS), and H_2O_2 exhibited significant mutagenicity in Endo III/VIII-deficient strains, i.e., YG3206 and YG3216, but not in the Endo III/VIII-proficient and FPG-deficient strains, i.e., YG3001 and YG3008 (Fig. 4). Phenazine ethosulfate (PES) exhibited mutagenicity only in YG3216 but not in YG3206 or the other strains. Thus, we categorized it into Group A′ (Table 3).

Group B compounds: Potassium bromate, MB plus visible light with the S9 mix, NR plus visible light, and B[*a*]P plus visible light (Table 3, Fig. 4) were more mutagenic in YG3001 than TA1535 and YG3206. The presence of pKM101 enhanced the mutagenicity of all Group B compounds except potassium bromate (Table 3, Fig. 4B).

Group C compounds: The mutagenicity of Group C compounds was dependent on the presence of pKM101 (Table 3). In these cases, the mutagenicity appeared unrelated to glycosylase deficiency; some were more mutagenic in YG3216 and others were more mutagenic in TA100.

In addition, *N*-nitrosotaurocholic acid (*N*-NTCA) was significantly mutagenic independent of DNA glycosylase status and without pKM101. This chemical was placed in a separate group, Group D (Table 3).

Discussion

Genetically engineered Ames tester strains are useful tools in environmental genotoxicology because they provide both extreme sensitivity and mechanistic information (36,37). For example, *S. typhimurium* strains YG7104 and YG7108, in which the repair systems for DNA damage by alkylating agents are disrupted, are hypersensitive to alkylating agents such as methyl

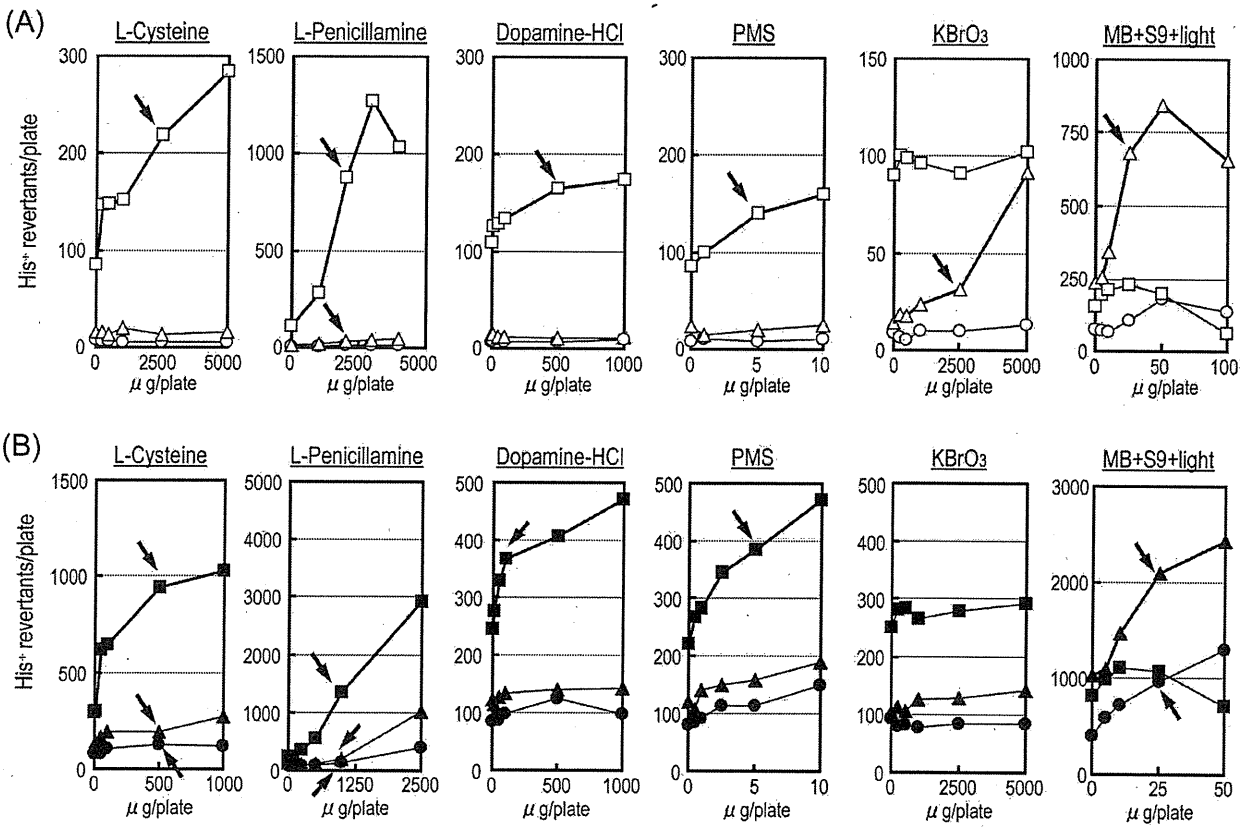

Fig. 4. Mutagenic responses of new *S. typhimurium* strains in the Ames test. The typical results for the test chemicals categorized into Groups A and B are indicated in (A) for the strains without pKM101 and (B) for the strains with pKM101 (Table 3). The number of His^+ revertants per plate was plotted against chemical dose in μg per plate. Symbols in (A): TA1535, ○; YG3001, △; YG3206, □. Symbols in (B): TA100, ●; YG3008, ▲; YG3216, ■. The arrows show the plot used for the calculation of the numbers shown in Table 3.

methanesulfonate and dimethylnitrosamine (38), and are used to investigate the mechanisms of chemical mutagenesis by this class of compounds (39,40). To expand the range of this research approach, we also established *S. typhimurium* strain YG5185, which can detect genotoxic PAHs with high specificity and sensitivity (41).

In the present study, we constructed strains YG3206 and YG3216, both of which lack two DNA glycosylases active on oxidized DNA pyrimidines. During the characterization of these strains, we noted that YG3206 exhibited specific sensitivity to the mutagenicity of L-cysteine; L-penicillamine; that is, dimethy L-cysteine; and dopamine-HCl. It is interesting that such naturally occurring compounds in organisms showed positive responses in the Ames tester strain. Similar findings have already been reported (42–44). Glatt reported the mutagenicity of L-cysteine and glutathione (GSH) in TA97, TA92, and TA104 with metabolic activation (42). Because the strains are not particularly sensitive to ROS, and catalase and superoxide dismutase did not inhibit the mutagenicity of GSH in TA92, Glatt concluded that ROS are not the cause of the L-cysteine and GSH mutagenicity. Our finding that YG3001 is not sensitive to the L-cysteine mutagenicity also suggests that high levels of 8-OH-G were not induced by cysteine. On the other hand, it has been reported that the mutagenicity of GSH and L-cysteine is oxidative in nature and involves ROS and/or other free radicals (43). Stark *et al.* proposed a mechanism for thiol mutagenesis: cysteine is converted to thiyl compounds, which react with transition metals and molecular oxygen and lead to produce H_2O_2 (43). Interestingly, H_2O_2 exhibited a similar pattern of mutagenicity with the tester strains as cysteine under our experimental conditions (Table 3). Both chemicals displayed mutagenicity in strain YG3206 but not TA1535 and YG3001, and the mutagenicity was enhanced by the introduction of pKM101. Therefore, it may be possible that cysteine generates H_2O_2, thereby oxidizing pyrimidines in DNA, which leads to mutations. Because we examined the mutagenicity of cysteine in the absence of S9 mix, the mechanism of mutation induction by cysteine may be different from those proposed by Glatt, who used S9 mix for the mutagenici-

ty assays of cysteine and GSH. Obviously, further work is needed to fully understand the mechanisms underlying the mutagenicity of cysteine and other chemicals in Group A.

As previously reported (29), H_2O_2 was not mutagenic in YG3001, a *mutM*$_{ST}$-deficient derivative of strain TA1535, but it was mutagenic in YG3003, a *mutM*$_{ST}$-deficient derivative of strain TA102. The reason that H_2O_2 was mutagenic in strain YG3003 is, perhaps, that the strain has an A:T base pair as its reversion target on multi-copy-number plasmid pAQ1. H_2O_2 exhibited mutagenicity in YG3206, which lacks both Endo III and Endo VIII activities (Table 3). Therefore, we suggest that H_2O_2 mainly induces oxidized pyrimidines in DNA. It may be interesting to construct a strain deficient in *nth*$_{ST}$ and *nei*$_{ST}$ and has an A:T base pair as a target for sensitive detection of H_2O_2 mutagenicity. Another noted result for H_2O_2 is that the introduction of pKM101 enhanced mutagenicity, even in the backgrounds of TA1535 and YG3001 (Table 3). The plasmid pKM101 encodes DNA polymerase, pol R1, which bypasses a variety of DNA lesions, including an abasic site, in efficiency (45). It may be possible that H_2O_2 induces lesions in DNA, for example an abasic site, which needs pol R1 to bypass it for mutagenesis. Collectively, our results suggest that H_2O_2 induces at least two types of lesions in DNA; one is oxidized pyrimidines that can be bypassed by endogenous *Salmonella* DNA polymerases for mutagenesis, and the other is abasic-site-like lesions that require the participation of pol R1 for mutagenesis.

The effect of visible light on chemical mutagenicity was observed for MB and NR. These chemicals have been reported to be more mutagenic in YG3001 than TA1535 (29). In this study, MB and NR, as well as B[*a*]P, exhibited higher mutagenicity in FPG-deficient strains than other strains, confirming the previous results. B[*a*]P usually requires metabolic activation to be mutagenic in *Salmonella*, but visible light activates it without metabolic activation (29). In the absence of irradiation, none of these chemicals was detectably mutagenic, even in YG3001 (data not shown). This observation is consistent with the proposed photodynamic generation of 8-OH-dG in DNA (46).

Our *nth* mutants exhibited a mild mutator phenotype, whereas the *nei* mutants had a spontaneous mutation frequency similar to wild-type cells. The *nth nei* double mutant, YG3206, exhibited a 20-fold increase in spontaneous mutation frequency (Fig. 3). This frequency is consistent with reports for analogous strains of *E. coli* (47,48). Considering the results shown above, L-cysteine and/or H_2O_2 may be candidates for increasing the spontaneous mutation frequency in YG3206. In addition, exposure to fluorescent light enhanced the mutation frequency. There may be certain endogenous chromophores that generate 8-OH-dG in DNA via photodynamic action.

Mammalian cells encode two Endo III-type glycosylases that recognize oxidative lesions. One of these, NTH1, removes a wide variety of oxidized pyrimidine derivatives, including thymine glycol and Fapy-dG (49–52). Knockout *Nth1* mice are reported to remain healthy (53,54). Three human genes, designated *NEIL1*, *NEIL2*, and *NEIL3*, encode proteins that contain sequence homologies to Endo VIII and FPG of *E. coli* (55–58). Inactivating mutations in *NEIL1* have been reported to correlate with human gastric cancer (59). In addition, RNA interference knockdown experiments in which a nearly 80% reduction in the *NEIL1* mRNA levels was achieved significantly sensitized cells to the killing effects of ionizing radiation (60). These data emphasize the importance of persistent oxidized pyrimidines in DNA. Taking into consideration the mutagenic effects of endogenous substances such as L-cysteine and H_2O_2, a possible critical role for *NEIL1* can be the exclusion of such endogenous mutagenic lesions, i.e., oxidized pyrimidines, for the long-term maintenance of genetic integrity.

In summary, we constructed a novel *S. typhimurium* strain, YG3206, by introducing *nth*$_{ST}$/*nei*$_{ST}$ deficiencies into the standard TA1535 Ames tester strain. The newly constructed strain exhibited higher specific sensitivity against chemicals that can be the cause of oxidized DNA pyrimidines. In particular, the strain detected the mutagenicity of naturally-occurring substances, such as L-cysteine, and suggested a possible involvement in spontaneous mutagenesis. We propose the combined use of YG3206 and YG3001 strains as a useful approach for mechanism-directed research of oxidative DNA damage.

Acknowledgements: The authors thank Dr. Peter Karran, Clare Hall Laboratories, Cancer Research, UK, London Research Institute, for critically reading the manuscript and his useful discussion. We also thank Drs. Toshihiro Ohta, Yukari Totsuka, and Kazuaki Kawai for generously providing precious chemicals. This work was supported in part by Grant-in-Aids for Cancer Research (19S-1) and for Scientific Research from the Ministry of Health, Labour, and Welfare of Japan.

References

1 Barnes DE, Lindahl T. Repair and genetic consequences of endogenous DNA base damage in mammalian cells. Annu Rev Genet. 2004; 38: 445–76.
2 Baute J, Depicker A. Base excision repair and its role in maintaining genome stability. Crit Rev Biochem Mol Biol. 2008; 43: 239–76.
3 Jackson AL, Chen R, Loeb LA. Induction of microsatellite instability by oxidative DNA damage. Proc Natl Acad

Sci USA. 1998; 95: 12468–73.
4 Ames BN, Shigenaga MK, Hagen TM. Oxidants, antioxidants, and the degenerative diseases of aging. Proc Natl Acad Sci USA. 1993; 90: 7915–22.
5 Cadet J, Douki T, Ravanat JL. Oxidatively generated damage to the guanine moiety of DNA: mechanistic aspects and formation in cells. Acc Chem Res. 2008; 41: 1075–83.
6 Friedberg EC, McDaniel LD, Schultz RA. The role of endogenous and exogenous DNA damage and mutagenesis. Curr Opin Genet Dev. 2004; 14: 5–10.
7 Dizdaroglu M. Oxidative damage to DNA in mammalian chromatin. Mutat Res. 1992; 275: 331–42.
8 Kasai H. Chemistry-based studies on oxidative DNA damage: formation, repair, and mutagenesis. Free Radic Biol Med. 2002; 33: 450–6.
9 Kasai H. Analysis of a form of oxidative DNA damage, 8-hydroxy-2′-deoxyguanosine, as a marker of cellular oxidative stress during carcinogenesis. Mutat Res. 1997; 387: 147–63.
10 Avkin S, Livneh Z. Efficiency, specificity and DNA polymerase-dependence of translesion replication across the oxidative DNA lesion 8-oxoguanine in human cells. Mutat Res. 2002; 510: 81–90.
11 Einolf HJ, Guengerich FP. Fidelity of nucleotide insertion at 8-oxo-7,8-dihydroguanine by mammalian DNA polymerase delta. Steady-state and pre-steady-state kinetic analysis. J Biol Chem. 2001; 276: 3764–71.
12 Haracska L, Prakash S, Prakash L. Yeast DNA polymerase zeta is an efficient extender of primer ends opposite from 7,8-dihydro-8-oxoguanine and O^6-methylguanine. Mol Cell Biol. 2003; 23: 1453–9.
13 Shibutani S, Takeshita M, Grollman AP. Insertion of specific bases during DNA synthesis past the oxidation-damaged base 8-oxodG. Nature. 1991; 349: 431–4.
14 Fowler RG, White SJ, Koyama C, Moore SC, Dunn RL, Schaaper RM. Interactions among the *Escherichia coli mutT*, *mutM*, and *mutY* damage prevention pathways. DNA Repair (Amst). 2003; 2: 159–73.
15 Boiteux S, Gajewski E, Laval J, Dizdaroglu M. Substrate specificity of the *Escherichia coli* Fpg protein (formamidopyrimidine-DNA glycosylase): excision of purine lesions in DNA produced by ionizing radiation or photosensitization. Biochemistry. 1992; 31: 106–10.
16 Michaels ML, Pham L, Cruz C, Miller JH. MutM, a protein that prevents G C→T A transversions, is formamidopyrimidine-DNA glycosylase. Nucleic Acids Res. 1991; 19: 3629–32.
17 Kreutzer DA, Essigmann JM. Oxidized, deaminated cytosines are a source of C→T transitions in vivo. Proc Natl Acad Sci USA. 1998; 95: 3578–82.
18 Shen JC, Rideout WM, III, Jones PA. The rate of hydrolytic deamination of 5-methylcytosine in double-stranded DNA. Nucleic Acids Res. 1994; 22: 972–6.
19 Jones PA, Rideout WM, III, Shen JC, Spruck CH, Tsai YC. Methylation, mutation and cancer. Bioessays. 1992; 14: 33–6.
20 Krokan HE, Nilsen H, Skorpen F, Otterlei M, Slupphaug G. Base excision repair of DNA in mammalian cells. FEBS Lett. 2000; 476: 73–7.
21 Melamede RJ, Hatahet Z, Kow YW, Ide H, Wallace SS. Isolation and characterization of endonuclease VIII from *Escherichia coli*. Biochemistry. 1994; 33: 1255–64.
22 Hatahet Z, Kow YW, Purmal AA, Cunningham RP, Wallace SS. New substrates for old enzymes. 5-Hydroxy-2′-deoxycytidine and 5-hydroxy-2′-deoxyuridine are substrates for *Escherichia coli* endonuclease III and formamidopyrimidine DNA *N*-glycosylase, while 5-hydroxy-2′-deoxyuridine is a substrate for uracil DNA *N*-glycosylase. J Biol Chem. 1994; 269: 18814–20.
23 Demple B, Harrison L. Repair of oxidative damage to DNA: enzymology and biology. Annu Rev Biochem. 1994; 63: 915–48.
24 Lindahl T. Repair of intrinsic DNA lesions. Mutat Res. 1990; 238: 305–11.
25 Wallace SS. DNA damages processed by base excision repair: biological consequences. Int J Radiat Biol. 1994; 66: 579–89.
26 Evans J, Maccabee M, Hatahet Z, Courcelle J, Bockrath R, Ide H, *et al.* Thymine ring saturation and fragmentation products: lesion bypass, misinsertion and implications for mutagenesis. Mutat Res. 1993; 299: 147–56.
27 Feig DI, Sowers LC, Loeb LA. Reverse chemical mutagenesis: identification of the mutagenic lesions resulting from reactive oxygen species-mediated damage to DNA. Proc Natl Acad Sci USA. 1994; 91: 6609–13.
28 Purmal AA, Kow YW, Wallace SS. Major oxidative products of cytosine, 5-hydroxycytosine and 5-hydroxyuracil, exhibit sequence context-dependent mispairing in vitro. Nucleic Acids Res. 1994; 22: 72–8.
29 Suzuki M, Matsui K, Yamada M, Kasai H, Sofuni T, Nohmi T. Construction of mutants of *Salmonella typhimurium* deficient in 8-hydroxyguanine DNA glycosylase and their sensitivities to oxidative mutagens and nitro compounds. Mutat Res. 1997; 393: 233–46.
30 Martínez A, Urios A, Blanco M. Mutagenicity of 80 chemicals in *Escherichia coli* tester strains IC203, deficient in OxyR, and its *oxyR*$^+$ parent WP2 *uvrA*/pKM101: detection of 31 oxidative mutagens. Mutat Res. 2000; 467: 41–53.
31 Levin DE, Hollstein M, Christman MF, Schwiers EA, Ames BN. A new Salmonella tester strain (TA102) with A X T base pairs at the site of mutation detects oxidative mutagens. Proc Natl Acad Sci USA. 1982; 79: 7445–9.
32 Maron DM, Ames BN. Revised methods for the Salmonella mutagenicity test. Mutat Res. 1983; 113: 173–215.
33 Link AJ, Phillips D, Church GM. Methods for generating precise deletions and insertions in the genome of wild-type *Escherichia coli*: application to open reading frame characterization. J Bacteriol. 1997; 179: 6228–37.
34 Yamada M, Hakura A, Sofuni T, Nohmi T. New method for gene disruption in *Salmonella typhimurium*: construction and characterization of an *ada*-deletion derivative of *Salmonella typhimurium* TA1535. J Bacteriol. 1993; 175: 5539–47.
35 Katafuchi A, Nakano T, Masaoka A, Terato H, Iwai S, Hanaoka F, *et al.* Differential specificity of human and

Escherichia coli endonuclease III and VIII homologues for oxidative base lesions. J Biol Chem. 2004; 279: 14464-71.
36 Josephy PD, Gruz P, Nohmi T. Recent advances in the construction of bacterial genotoxicity assays. Mutat Res. 1997; 386: 1-23.
37 Nohmi T. Novel DNA polymerases and novel genotoxicity assays. Genes Environ. 2007; 29: 75-88.
38 Yamada M, Sedgwick B, Sofuni T, Nohmi T. Construction and characterization of mutants of *Salmonella typhimurium* deficient in DNA repair of O^6-methylguanine. J Bacteriol. 1995; 177: 1511-9.
39 Ishikawa S, Mochizuki M. Mutagenicity and cross-linking activity of chloroalkylnitrosamines, possible new antitumor lead compounds. Mutagenesis. 2003; 18: 331-5.
40 Okochi E, Namai E, Ito K, Mochizuki M. Activation of *N*-nitrosodialkylamines to mutagens by a metalloporphyrin/oxidant model system for cytochrome P450. Biol Pharm Bull. 1995; 18: 49-52.
41 Yamada M, Matsui K, Nohmi T. Development of a bacterial hyper-sensitive tester strain for specific detection of the genotoxicity of polycyclic aromatic hydrocarbons. Genes Environ. 2006; 28: 23-30.
42 Glatt H. Mutagenicity spectra in *Salmonella typhimurium* strains of glutathione, L-cysteine and active oxygen species. Mutagenesis. 1989; 4: 221-7.
43 Stark AA, Pagano DA, Glass G, Kamin-Belsky N, Zeiger E. The effects of antioxidants and enzymes involved in glutathione metabolism on mutagenesis by glutathione and L-cysteine. Mutat Res. 1994; 308: 215-22.
44 Glatt H, Protic-SabljiC M, Oesch F. Mutagenicity of glutathione and cysteine in the Ames test. Science. 1983; 220: 961-3.
45 Goldsmith M, Sarov-Blat L, Livneh Z. Plasmid-encoded MucB protein is a DNA polymerase (pol RI) specialized for lesion bypass in the presence of MucA′, RecA, and SSB. Proc Natl Acad Sci USA. 2000; 97: 11227-31.
46 Kim SR, Kokubo K, Matsui K, Yamada N, Kanke Y, Fukuoka M, *et al.* Light-dependent mutagenesis by benzo[*a*]pyrene is mediated via oxidative DNA damage. Environ Mol Mutagen. 2005; 46: 141-9.
47 Jiang D, Hatahet Z, Blaisdell JO, Melamede RJ, Wallace SS. *Escherichia coli* endonuclease VIII: cloning, sequencing, and overexpression of the nei structural gene and characterization of *nei* and *nei nth* mutants. J Bacteriol. 1997; 179: 3773-82.
48 Saito Y, Uraki F, Nakajima S, Asaeda A, Ono K, Kubo K, *et al.* Characterization of endonuclease III (*nth*) and endonuclease VIII (*nei*) mutants of *Escherichia coli* K-12. J Bacteriol. 1997; 179: 3783-5.
49 Asagoshi K, Odawara H, Nakano H, Miyano T, Terato H, Ohyama Y, *et al.* Comparison of substrate specificities of *Escherichia coli* endonuclease III and its mouse homologue (mNTH1) using defined oligonucleotide substrates. Biochemistry. 2000; 39: 11389-98.
50 Dizdaroglu M, Karahalil B, Senturker S, Buckley TJ, Roldan-Arjona T. Excision of products of oxidative DNA base damage by human NTH1 protein. Biochemistry. 1999; 38: 243-6.
51 Aspinwall R, Rothwell DG, Roldan-Arjona T, Anselmino C, Ward CJ, Cheadle JP, *et al.* Cloning and characterization of a functional human homolog of *Escherichia coli* endonuclease III. Proc Natl Acad Sci USA. 1997; 94: 109-14.
52 Hilbert TP, Boorstein RJ, Kung HC, Bolton PH, Xing D, Cunningham RP, *et al.* Purification of a mammalian homologue of *Escherichia coli* endonuclease III: identification of a bovine pyrimidine hydrate-thymine glycol DNAse/AP lyase by irreversible cross linking to a thymine glycol-containing oligoxynucleotide. Biochemistry. 1996; 35: 2505-11.
53 Ocampo MT, Chaung W, Marenstein DR, Chan MK, Altamirano A, Basu AK, *et al.* Targeted deletion of *mNth1* reveals a novel DNA repair enzyme activity. Mol Cell Biol. 2002; 22: 6111-21.
54 Takao M, Kanno S, Shiromoto T, Hasegawa R, Ide H, Ikeda S, *et al.* Novel nuclear and mitochondrial glycosylases revealed by disruption of the mouse *Nth1* gene encoding an endonuclease III homolog for repair of thymine glycols. EMBO J. 2002; 21: 3486-93.
55 Bandaru V, Sunkara S, Wallace SS, Bond JP. A novel human DNA glycosylase that removes oxidative DNA damage and is homologous to *Escherichia coli* endonuclease VIII. DNA Repair (Amst). 2002; 1: 517-29.
56 Hazra TK, Izumi T, Boldogh I, Imhoff B, Kow YW, Jaruga P, *et al.* Identification and characterization of a human DNA glycosylase for repair of modified bases in oxidatively damaged DNA. Proc Natl Acad Sci USA. 2002; 99: 3523-8.
57 Morland I, Rolseth V, Luna L, Rognes T, Bjoras M, Seeberg E. Human DNA glycosylases of the bacterial Fpg/MutM superfamily: an alternative pathway for the repair of 8-oxoguanine and other oxidation products in DNA. Nucleic Acids Res. 2002; 30: 4926-36.
58 Takao M, Kanno S, Kobayashi K, Zhang QM, Yonei S, van der Horst GT, *et al.* A back-up glycosylase in *Nth1* knock-out mice is a functional Nei (endonuclease VIII) homologue. J Biol Chem. 2002; 277: 42205-13.
59 Shinmura K, Tao H, Goto M, Igarashi H, Taniguchi T, Maekawa M, *et al.* Inactivating mutations of the human base excision repair gene *NEIL1* in gastric cancer. Carcinogenesis. 2004; 25: 2311-7.
60 Rosenquist TA, Zaika E, Fernandes AS, Zharkov DO, Miller H, Grollman AP. The novel DNA glycosylase, NEIL1, protects mammalian cells from radiation-mediated cell death. DNA Repair (Amst). 2003; 2: 581-91.

Chem. Res. Toxicol. **2010,** *23,* 630–636

DNA Modifications by the ω-3 Lipid Peroxidation-Derived Mutagen 4-Oxo-2-hexenal in Vitro and Their Analysis in Mouse and Human DNA

Kazuaki Kawai,[†] Pei-Hsin Chou,[‡] Tomonari Matsuda,[‡] Masaaki Inoue,[§] Kaisa Aaltonen,[||] Kirsti Savela,[||] Yoshikazu Takahashi,[⊥] Hikaru Nakamura,[⊥] Tomoyuki Kimura,[⊥] Takumi Watanabe,[⊥] Ryuichi Sawa,[⊥] Kazuyuki Dobashi,[#] Yun-Shan Li,[†] and Hiroshi Kasai*[,†]

Department of Environmental Oncology, Institute of Industrial Ecological Sciences, University of Occupational and Environmental Health, 1-1, Iseigaoka, Yahatanishi-ku, Kitakyushu, 807-8555, Japan, Research Center for Environmental Quality Management, Kyoto University, 1-2 Yumihama, Otsu, Shiga, 520-0811, Japan, Department of Chest Surgery, Niigata Rosai Hospital, 1-7-12 Touncho, Joetsu, Niigata, 942-8502, Japan, Risk Assessment Unit, Finnish Food Safety Authority Evira, Mustialankatu 3, FI-00790 Helsinki, Finland, Microbial Chemistry Research Center, 3-14-23, Kamiosaki, Shinagawa-ku, Tokyo, 141-0021, Japan, and Japan Bioindustry Association, Grande Building 8F, 2-26-9 Hatchobori, Chuo-ku, Tokyo 104-0032, Japan

Received October 16, 2009

4-Oxo-2-hexenal (4-OHE), which forms a 2′-deoxyguanosine (dG) adduct in a model lipid peroxidation system, is mutagenic in the Ames test. It is generated by the oxidation of ω-3 fatty acids and is commonly found in dietary fats, such as fish oil, perilla oil, rapeseed oil, and soybean oil. 4-OHE also forms adducts with 2′-deoxyadenosine (dA), 2′-deoxycytidine (dC), and 5-methyl-2′-deoxycytidine (5-Me-dC) in DNA. In this study, we characterized the structures of these adducts in detail. We measured the amounts of 4-OHE−DNA adducts in mouse organs by LC/MS/MS, after 4-OHE was orally administered to mice. The 4-OHE−dA, 4-OHE−dC, 4-OHE−dG, and 4-OHE−5-Me-dC adducts were detected in stomach and intestinal DNA in the range of 0.25−43.71/10^8 bases. After the 4-OHE administration, the amounts of these DNA adducts decreased gradually over 7 days. We also detected 4-OHE−dC in human lung DNA, in the range of 2.6−5.9/10^9 bases. No difference in the 4-OHE adduct levels was detected between smokers and nonsmokers. Our results suggest that 4-OHE−DNA adducts are formed by endogenous as well as environmental lipid peroxides.

Introduction

The oxidation of unsaturated fatty acids generates toxic reactive aldehydes, such as 4-hydroxy-2-nonenal, malondialdehyde, acrolein, and crotonaldehyde (*1*−*3*). These aldehydes directly react with DNA and are considered to contribute to mutagenesis and carcinogenesis (*4*−*6*). Unsaturated aldehydes are generated not only as pollutants by heat decomposition of fat (*7*), cigarette smoking (*8*), and other environmental factors but also as oxidation products of membrane lipids in vivo (*9*). Although the exact mechanism is not clear, these environmental and endogenous aldehydes may play a role in tissue toxicity and carcinogenicity. Recently, we found a novel mutagenic oxidation product, 4-oxo-2-hexenal (4-OHE),[1] in the lipid peroxidation model reaction (*10*−*13*). Namely, when dG was reacted with linolenic acid methyl ester and Fe-containing hemin, as a catalyst for lipid peroxidation, six dG adducts were detected by an HPLC analysis. One of them was the 4-OHE−dG adduct (dG*), and thus 4-OHE was considered to be a new mutagen produced by ω-3 lipid peroxidation. 4-OHE is mutagenic in the *Salmonella typhimurium* strains TA 104 and TA 100, and it covalently modifies dC, dG, and 5-Me-dC to form substituted etheno type adducts. Our new results revealed that 4-OHE could also modify dA to produce an etheno-dA derivative. These 4-OHE adducts were detected after DNA was treated with 4-OHE in vitro. These results are basically similar to those from structural studies on adduct formation by 4-oxo-2-nonenal with DNA or nucleosides in vitro (*14*−*17*).

Because the diet plays a pivotal role in the development of human cancer (*18*), it is important to identify whether this novel mutagen, 4-OHE, exists in foods. Actually, 4-OHE was present in commercial perilla oil, the edible part of broiled fish, and various fried foods in the range of 1−70 μg/g (*12*). Furthermore, 4-OHE was detected by a GC/MS analysis of the ethyl acetate trap of the smoke released during the broiling of fish. Some epidemiological and experimental studies have demonstrated that cooking oil vapors may be related to cancer risk (*19, 20*). In general, these types of DNA adducts are considered as promutagenic lesions and can lead to the initiation of carcinogenesis. The detection and quantitation of these adducts as markers for the initiation of cancer may be useful for cancer risk assessment. The in vivo formation of the DNA adducts of 4-OHE has not

* To whom correspondence should be addressed. Tel: +81-93-691-7469. Fax: +81-93-601-2199. E-mail: h-kasai@med.uoeh-u.ac.jp.
[†] University of Occupational and Environmental Health.
[‡] Kyoto University.
[§] Niigata Rosai Hospital.
[||] Finnish Food Safety Authority Evira.
[⊥] Microbial Chemistry Research Center.
[#] Japan Bioindustry Association.

[1] Abbreviations: 4-OHE, 4-oxo-2-hexenal; HRESI-MS, high-resolution electrospray ionization mass spectrometry; ESI-MS, electrospray ionization mass spectrometry; FAB-MS, fast atom bombardment mass spectrometry; ORTEP, Oak Ridge Thermal Ellipsoid Program; COSY, correlation spectroscopy; HMQC, heteronuclear multiple quantum correlation; HMBC, heteronuclear multiple bond correlation; NOESY, nuclear Overhauser effect spectroscopy.

10.1021/tx9003819
Published on Web 01/07/2010

previously been demonstrated, except in our previous brief report (*10*). In the present study, we report the detailed structural characterization of the 4-OHE–dA, 4-OHE–dC, and 4-OHE–5-Me-dC adducts and the detection of 4-OHE adducts in the organ DNA from 4-OHE-exposed mice and in human lung DNA by an LC/MS/MS method.

Materials and Methods

Materials. Deoxycytidine hydrochloride and deoxyadenosine were obtained from Yoshitomi Pharmaceutical Co., which is presently Yoshitomiyakuhin Co. (Osaka, Japan). 5-Methyl-2′-deoxycytidine and 2′-deoxycytidine 3′-monophosphate sodium salt were purchased from Sigma Chemical Co. (St. Louis, MO). Stable isotope-labeled compounds, 2′-deoxyadenosine (U-$^{15}N_5$, 98%) and 2′-deoxycytidine (U-$^{15}N_3$, 96–98%), were obtained from Cambridge Isotope Laboratories, Inc. (MA). 4-OHE was synthesized according to a previously described method (*11*).

Spectra Measurements. The mass spectra of the adducts were recorded with JEOL JMS-DX-303 (fast atom bombardment mass spectrometry, FAB-MS), JEOL JMS-T100LC (electrospray ionization mass spectrometry, ESI-MS), and Thermo Fisher Scientific LTQ Orbitrap (ESI-MS/MS) mass spectrometers. ^{1}H and ^{13}C NMR spectra were measured with a JEOL JNM-ECA600 spectrometer, using tetramethylsilane (TMS) as an internal reference.

X-ray Crystallography of 4-OHE-dC (dC*). A colorless prismatic crystal of dC*, with approximate dimensions of 0.40 mm × 0.10 mm × 0.05 mm, was chosen for X-ray crystallography. The crystal data are as follows: empirical formula, $C_{15}H_{19}N_3O_5$; FW, 321.33; crystal system, orthorhombic; lattice parameters: a = 8.4034 (13) Å, b = 34.9581 (18) Å, c = 5.1410 (17) Å, and V = 1510.3 (6) Å^3; space group, $P2_12_12_1$; Z value, 4; D_{calcd}, 1.413 g/cm^3; and μ(Cu Kα), 9.027 cm^{-1}. X-ray crystallographic measurements were performed on a Rigaku AFC7R diffractometer, with graphite monochromated Cu Kα radiation and a rotating anode generator. Data processing was performed using CrystalStructure 3.8.2 (Rigaku).

Preparation of 8-(2-Oxobutyl)-3,*N*4-etheno-dC (dC*). Deoxycytidine hydrochloride (52.8 mg, 0.200 mmol) and 4-OHE (67.2 mg, 0.599 mmol) were dissolved in 24 mL of 50 mM sodium phosphate buffer (pH 7.4) containing 10% ethanol and incubated for 5 days at room temperature. The product (retention time, 42.5–43.6 min) was separated by repeated rounds of HPLC [column: CAPCELL PAK C18, 5 μm, 10 mm × 250 mm, Shiseido Fine Chemicals, Japan; elution: 0–40 min, linear gradient of methanol (15–30%); 40–60 min, 30% methanol; flow rate, 3 mL/min]. The yield was 20.5 mg (32.0%).

Preparation of 8-(2-Oxobutyl)-3,*N*4-etheno-5-methyl-dC (5-Me-dC*). 5-Methyl-2′deoxycytidine (50.3 mg, 0.209 mmol) and 4-OHE (25.8 mg, 0.230 mmol) were dissolved in 25 mL of 50 mM sodium acetate (pH 5.0) containing 10% ethanol and incubated for 5 days at room temperature. The product (retention time, 52.4–54.2 min) was separated by repeated rounds of HPLC (the same conditions as above). The yield was 28.8 mg (41.0%).

Preparation of 11-(2-Oxobutyl)-1,*N*6-etheno-dA (dA*). Deoxyadenosine (100 mg, 0.398 mmol) and 4-OHE (126 mg, 1.124 mmol) were dissolved in 100 mL of 5% aqueous ethanol and incubated for 15 h at 50 °C. The product (retention time, 33.7–35.5 min) was separated by repeated rounds of HPLC (column: CAPCELL PAK C18, 5 μm, 10 mm × 250 mm; elution: 12% aqueous acetonitrile; flow rate, 3 mL/min). The yield was 20.0 mg (14.5%).

Preparation of Isotope-Labeled dC* and dA*. Stable isotope-labeled dC* and dA* were prepared from 2′-deoxyadenosine (U-$^{15}N_5$, 98%) and 2′-deoxycytidine (U-$^{15}N_3$, 96–98%) by a similar procedure as described above. Briefly, ^{15}N-deoxycytidine (5 mg) and 4-OHE (8 mg) were dissolved in 1 mL of 50 mM sodium phosphate buffer (pH 7.4) containing 10% ethanol and incubated for 3 days at room temperature. The product ^{15}N-dC* (retention time, 27.2 min) was separated by repeated rounds of HPLC [column: CAPCELL PAK C18, 5 μm, 4.6 mm × 250 mm; elution: 0–30 min, linear gradient of methanol (15–30%); flow rate, 1 mL/min]. For the preparation of ^{15}N-dA*, ^{15}N-deoxyadenosine (5.8 mg) and 4-OHE (10 mg) were dissolved in 1 mL of 10% aqueous ethanol and incubated for 10 h at 50 °C. The product (retention time, 20.6 min) was separated by repeated rounds of HPLC (column: CAPCELL PAK C18, 5 μm, 4.6 mm × 250 mm; elution: 12% aqueous acetonitrile; flow rate, 1 mL/min).

Reaction of 4-OHE with Calf Thymus DNA in Vitro. 4-OHE (5 μL) was added to calf thymus DNA (1 mg, heat denatured in boiling water for 10 min) in 1 mL of phosphate buffer (50 mM, pH 7.0) containing 17% ethanol. The reaction mixture was incubated at 37 °C for 16 h. The DNA was precipitated by adding 2.4 mL of cold ethanol and 20 mL of cold 2 M sodium acetate. After the solution was centrifuged, the supernatant was removed, and the DNA pellet was washed with 1 mL of cold 70% ethanol. The DNA pellet was dried under reduced pressure.

Hydrolysis of 4-OHE-Modified Calf Thymus DNA. The modified DNA was dissolved in 0.3 mL of water. A 100 μL aliquot of 0.5 M Tris-HCl (pH 8.0) and 5 mM $MgCl_2$, 3 μL of snake venom phosphodiesterase I (100 units/mL, Funakoshi Co., Ltd., Tokyo, Japan), and 4 mL of alkaline phosphatase (1 u/μL, Roche Diagnostics Gmbh, Mannheim, Germany) were added to the DNA solution. The DNA was hydrolyzed at 37 °C overnight and filtered through a 0.45 μm filter before analysis by HPLC.

Treatment of Animals. Five week old female ICR mice were obtained from SLC Japan Inc. (Shizuoka, Japan). Animals were maintained in a temperature- and photoperiod (12 h/day)-controlled room. The animals were fed with the standard diet CE-2 from CLEA Japan Inc. (Tokyo). Oral doses of 3 mg 4-OHE/mouse dissolved in corn oil were administered i.g. to 6 week old female ICR mice. Control animals were treated with corn oil only. The mice were sacrificed under deep ether anesthesia at different times, ranging from 24 h to 7 days. Harvested were the following organs: esophagus, stomach, liver, kidney, small intestine, and large intestine. The digestive tract organs were washed with 70% ethanol and a sodium chloride solution. The organs were stored at −80 °C. All of the animal experimental procedures were performed in accordance with the guidelines for the care and use of laboratory animals at our university.

Preparation of Human Lung Tissues. Lung samples were obtained during surgery for 10 lung cancer patients at the Niigata Rosai Hospital (Niigata, Japan). After resection, noncancerous lung tissues were removed, frozen immediately in liquid nitrogen, and stored at −80 °C.

DNA Extraction. The nuclear DNA of the mouse tissue and the human lung was isolated by the sodium iodide method, using a DNA Extraction WB Kit (Wako Pure Chemical Industries, Ltd., Osaka, Japan). To avoid oxidative DNA artifacts, 1 mM desferal (deferoxamine mesylate, Sigma Chemical Co.) was added to the lysis solution for the tissue homogenization and DNA extraction. A 50 mg portion of tissue was homogenized with a Teflon glass homogenizer, in 1 mL of ice-cold lysis solution. Subsequent DNA isolation was performed according to the manufacturer's instructions.

DNA Hydrolysis. The isolated DNA was enzymatically digested as follows: Each DNA sample (50 μg for the mouse tissues and 25 μg for the human lung samples) was mixed with 36 μL of digestion buffer (17 mM sodium succinate and 8 mM calcium chloride, pH 6.0) containing 45 units of micrococcal nuclease (Worthington, United States), 0.15 units of spleen phosphodiesterase (Worthington), and two stable isotope internal standards, [$^{15}N_3$]-dC* (20 fmol) and [$^{15}N_5$]-dA* (20 fmol). After 3 h of incubation at 37 °C, 3 units of alkaline phosphatase (Sigma, United States), 10 μL of 0.5 M Tris-HCl (pH 8.5), 5 μL of 20 mM zinc sulfate, and 49 μL of Milli-Q water were added, and the mixture was incubated for 3 h at 37 °C. After this incubation, the mixture was concentrated to 10–20 μL by a Speed-Vac concentrator, and 100 μL of methanol was added to precipitate the protein. After centrifugation, the methanol fraction (supernatant) was transferred to a new Eppendorf tube. The precipitate was extracted with 100 μL of methanol, and the methanol fractions were combined and evaporated to dryness.

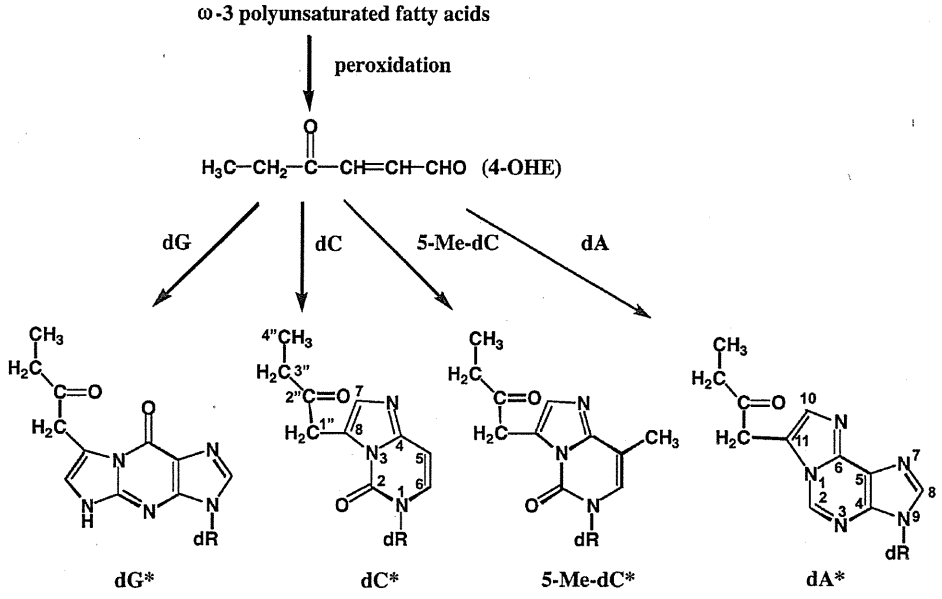

Figure 1. Structures of 4-OHE–DNA adducts.

Samples were resuspended in 50 μL of Milli-Q water before LC/ESI-MS/MS analysis.

LC/ESI-MS/MS Analyses. The LC/MS/MS analysis was performed using a Quattro Ultima Pt triple stage quadrupole mass spectrometer (Waters-Micromass, United States) equipped with a Shimadzu LC system (Shimadzu, Japan). An aliquot of each sample (40 μL) was injected and separated by a Shim-pack XR-ODS column (3.0 mm × 75 mm, Shimadzu, Japan). The column was eluted with a linear gradient of 15–80% methanol in water from 0 to 15 min at a flow rate of 0.2 mL/min and then was switched back to the initial condition of 15% methanol in water from 15 to 27 min. Mass spectral analysis was performed in the positive ion mode, using nitrogen as the nebulizing gas. Experimental conditions were set as follows: ion source temperature, 130 °C; desolvation temperature, 380 °C; cone voltage, 35 V; desolvation gas flow rate, 700 L/h; and cone gas flow rate, 35 L/h. Argon was used as the collision gas. The collision energy and characteristic reactions (base ion→product ion) monitored for the different DNA adducts are as follows: dC* (10 eV, 321.8→205.8), [$^{15}N_3$]-dC* (10 eV, 324.8→208.6), 5-Me-dC* (20 eV, 335.9→220.0), dA* (10 eV, 345.8→229.8), [$^{15}N_5$]-dA* (10 eV, 351.0→234.8), and dG* (20 eV, 362.0→245.9).

The amount of each DNA adduct was quantified by calculating the peak area ratio of the target DNA adduct and its specific internal standard ([$^{15}N_3$]-dC* was used for dC* and 5-Me-dC*, and [$^{15}N_5$]-dA* was used for dA* and dG*). Calibration curves were obtained using authentic standards spiked with isotopically labeled internal standards. The concentration of 2′-deoxyguanosine (dG) in each DNA sample was also monitored by the SPD-10Avp UV–visible detector in the Shimadzu LC system, and the adduct levels in each sample were calculated using the amount of dG. The number of DNA adducts per 10^9 bases was calculated by the following equation: number of DNA adducts per 10^9 bases = adduct level (fmol/μmol dG) × 0.218(μmol dG/μmol dN), as described previously (*21*).

The signal-to-noise ratio (S/N: peak to peak) of the adduct peak was calculated by using the Masslynx V4.0 software. The detection limits of the adducts, for which the peaks were expected to have an S/N of 3, were 0.13 (dG*), 0.35 (dA*), 0.41 (Me-dC*), and 0.08 fmol (dC*). This sensitivity was sufficient to detect 0.5–2.7 adducts per 10^9 bases when using 50 μg of DNA. The quantification limits of the peaks that were expected to have an S/N of 10 were also estimated to be 0.26 (dG*), 0.92 (dA*), 0.87 (Me-dC*), and 0.23 fmol (dC*).

Table 1. NMR Data of dC* in DMSO-d_6[a]

position	δ_C (ppm)	δ_H (ppm)	multiplicity, *J* (Hz)
2	146.8		
4	145.1		
5	98.9	6.62	d, 8.1
6	127.8	7.61	d, 8.1
7	132.6	7.11	s
8	123.0		
1′	84.7	6.30	t, 6.8
2′	40.0	2.14	m
3′	70.4	4.26	m
3′-OH		5.26	br
4′	87.6	3.81	q, 3.7
5′	61.2	3.56	dd, 3.7, 12.2
		3.60	dd, 3.7, 12.2
5′-OH		5.13	br
1″	38.7	4.11	d, 17.7
		4.15	d, 17.7
2″	206.7		
3″	34.5	2.54	q, 7.3
4″	7.6	0.95	t, 7.3

[a] Chemical shifts in ppm from TMS as an internal standard.

Results

Structure Confirmation of 4-OHE Adducts with dC, 5-Me-dC, and dA. 4-OHE reacts not only with dG but also with dC, 5-Me-dC, and dA to yield adducts (dC*, 5-Me-dC*, and dA*). The structures of dC*, 5-Me-dC*, and dA* were determined as shown in Figure 1, mainly by the MS, NMR, and X-ray crystallography data. ^1H and ^{13}C NMR data for these synthetic compounds are provided in Tables 1–3.

The molecular formula of dC* is consistent with $C_{15}H_{19}N_3O_5$, as determined by high-resolution electrospray ionization mass spectrometry (HRESI-MS) [positive ion mode, *m/z* 344.1192 $(M + Na)^+$ 344.1222 calcd for $C_{15}H_{19}N_3O_5Na$]. The HRESI-MS/MS spectrum of *m/z* 322.1 revealed product ions at *m/z* 206.0923 (Δ −0.11 mDa as $C_{10}H_{12}N_3O_2$: base + H_2), *m/z* 150.0659 (Δ −0.31 mDa $C_7H_8N_3O$: base + H_2 − C_2H_5CO), and *m/z* 121.0631 and *m/z* 57.0332 (Δ −0.25 mDa C_3H_5O: etheno ring side chain). The UV λ_{max} in H_2O was 277 nm (ε 11460). The ^1H and ^{13}C NMR spectra showed additional characteristic signals: CH_2 (δ_H 4.11 and 4.15, δ_C 38.7), C=O (δ_C 206.7), CH_2 (δ_H 2.54, δ_C 34.5), and CH_3 (δ_H 0.95, δ_C 7.6), as compared with those of dC (Table 1). dC* generated a highly

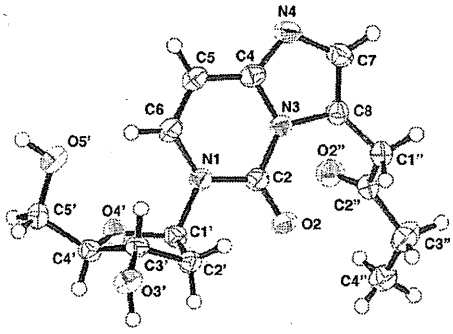

Figure 2. Crystal structure of dC*.

Table 2. NMR Data of 5-Me-dC* in DMSO-d_6[a]

position	δ_C (ppm)	δ_H (ppm)	multiplicity, J (Hz)
2	146.7		
4	146.0		
5	107.2		
5-CH_3	12.8	2.14	brd, 1.0
6	124.2	7.42	brq, 1.0
7	132.4	7.11	s
8	123.5		
1′	84.4	6.30	t, 6.8
2′	39.8	2.12	m
3′	70.4	4.26	m
3′-OH		5.26	d, 4.3
4′	87.5	3.79	dd, 3.7
5′	61.3	3.56	dt, 4.3, 12.1
		3.62	ddd, 3.7, 5.0, 12.1
5′-OH		5.06	t, 5.2
1″	38.7	4.10	d, 17.7
		4.15	d, 17.7
2″	206.7		
3″	34.5	2.53	q, 7.3
4″	7.6	0.95	t, 7.3

[a] Chemical shifts in ppm from TMS as an internal standard.

crystalline product, and thus, further structure elucidation was performed by X-ray crystallography. The compound was recrystallized by an ethanol:water (1:1) solvent system and yielded colorless prisms. An Oak Ridge Thermal Ellipsoid Program (ORTEP) drawing of dC* is shown in Figure 2. The sugar of dC* adopts the C(3′)-endo conformation, and the glycosidic torsion is in the anti form.

The molecular formula of 5-Me-dC* is consistent with $C_{16}H_{21}N_3O_5Na$, as determined by HRESI-MS [positive ion mode, m/z 358.1372, $(M + Na)^+$ 358.1379 calcd for $C_{15}H_{19}N_3O_5Na$]. The HRESI-MS/MS spectrum of m/z 336.2 revealed product ions at m/z 220.1079 (Δ −0.15 mDa as $C_{11}H_{14}N_3O_2$: base + H_2), m/z 164.0816 (Δ −0.26 mDa as $C_8H_{10}N_3O$: base + H_2 − C_2H_5CO), and m/z 135.0788, m/z 108.0679, and m/z 57.0333 (Δ −0.23 mDa as C_3H_5O: etheno ring side chain). The UV λ_{max} in H_2O was 278 nm (ε 11930). The ^1H and ^{13}C NMR spectra showed almost the same additional characteristic signals of dC*: CH_2 (δ_H 4.10 and 4.15, δ_C 38.7), C=O (δ_C 206.7), CH_2 (δ_H 2.53, δ_C 34.5), and CH_3 (δ_H 0.95, δ_C 7.6), as compared with those of 5-Me-dC (Table 2). Further structure determination was accomplished by various two-dimensional NMR techniques, such as correlation spectroscopy (COSY), heteronuclear multiple quantum correlation (HMQC), and heteronuclear multiple bond correlation (HMBC), as summarized in Figure 3. The 2-oxo-butyl side chain was attached to C-8 of the imidazole ring, as confirmed by $^1H-^{15}N$ HMBC, where cross-peaks were observed between H-1″ and N-3.

The molecular formula of dA* is consistent with $C_{16}H_{19}N_5O_4$, as determined by HRESI-MS [positive ion mode, m/z 368.1320, $(M + Na)^+$ 368.1329 calcd for $C_{16}H_{19}N_5O_4Na$]. The UV λ_{max}

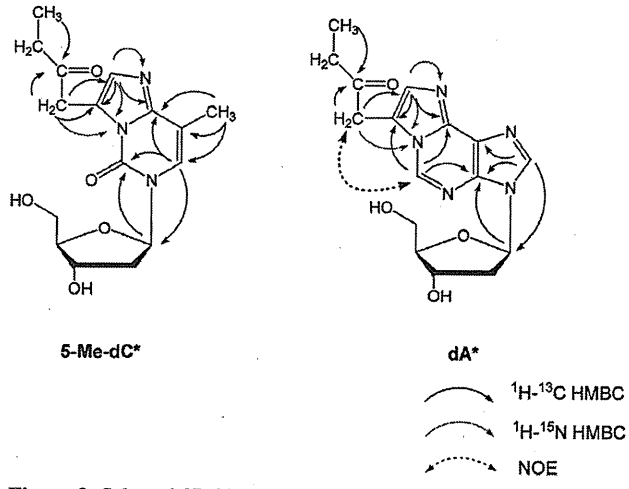

Figure 3. Selected 2D NMR results of 5-Me-dC* and dA*.

Table 3. NMR Data of dA* in DMSO-d_6[a]

position	δ_C (ppm)	δ_H (ppm)	multiplicity, J (Hz)
2	135.8	8.98	s
4	137.8		
5	123.1		
6	140.7		
8	139.8	8.51	s
10	131.8	7.34	s
11	118.5		
1′	84.0	6.47	t, 6.5
2′	39.7	2.36	ddd, 3.4, 6.5, 13.4
		2.75	dt, 6.5, 13.4
3′	70.7	4.44	m
3′-OH		5.35	d, 4.1
4′	88.0	3.89	dt, 3.1, 5.0
5′	61.7	3.54	dt, 5.0, 11.7
		3.63	dt, 5.0, 11.7
5′-OH		4.96	t, 5.0
1″	36.8	4.33	s
2″	206.7		
3″	34.5	2.65	q, 7.3
4″	7.5	0.97	t, 7.3

[a] Chemical shifts in ppm from TMS as an internal standard.

values in H_2O were 232 (ε 25800), 270 (ε 5980), and 279 nm (ε 6080). The HRESI-MS/MS spectrum of m/z 346.2 revealed product ions at m/z 230.1035 (Δ −0.18 mDa as $C_{11}H_{12}N_5O$: base + H_2) and m/z 173.0694 (Δ −0.17 mDa as $C_8H_7N_5$: base + H_2 − C_2H_5CO). The ^1H and ^{13}C NMR spectra showed additional characteristic signals: CH_2 (δ_H 4.33, δ_C 36.8), C=O (δ_C 206.7), CH_2 (δ_H 2.65, δ_C 34.5), and CH_3 (δ_H 0.97, δ_C 7.5), as compared with those of dA (Table 3). Further structure determination was accomplished by various two-dimensional NMR techniques, such as COSY, HMQC, HMBC, and nuclear Overhauser effect spectroscopy (NOESY), as summarized in Figure 3. The $^1H-^{13}C$ HMBC spectrum of dA* is shown in Figure 4. The 2-oxo-butyl side chain was attached to C-11 of the imidazole ring, as confirmed by a NOE observed between H-2 and H-1″, and the cross-peaks observed between H-1″ and N-1 by $^1H-^{15}N$ HMBC.

Reaction of 4-OHE with Calf Thymus DNA in Vitro. The 4-OHE−DNA adducts formed by the reaction of 4-OHE and calf thymus DNA in vitro were analyzed by HPLC (Figure 5). They were efficiently formed in heat-denatured calf thymus DNA (ss DNA). The yield of the 4-OHE−DNA adducts was about 50 times higher in ss DNA than in ds DNA (data not shown). At a physiological pH, the efficient formation of dC* and 5-Me-dC* was observed (Table 4). This may be due to the higher reactivity of 4-OHE with dC and 5-Me-dC than with dG and dA, rather than steric reasons.

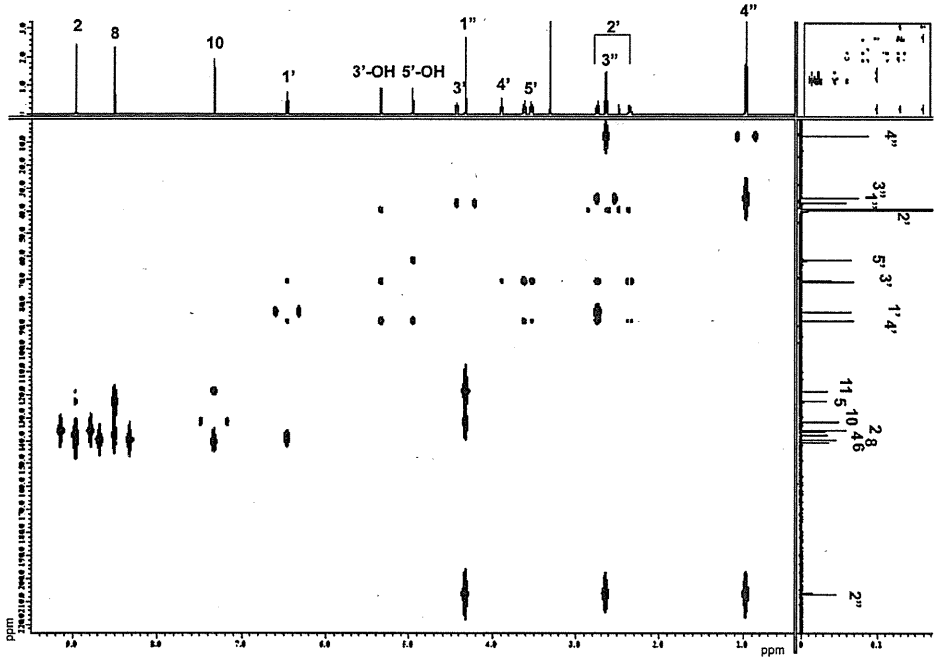

Figure 4. $^{1}H-^{13}C$ HMBC spectrum of dA*.

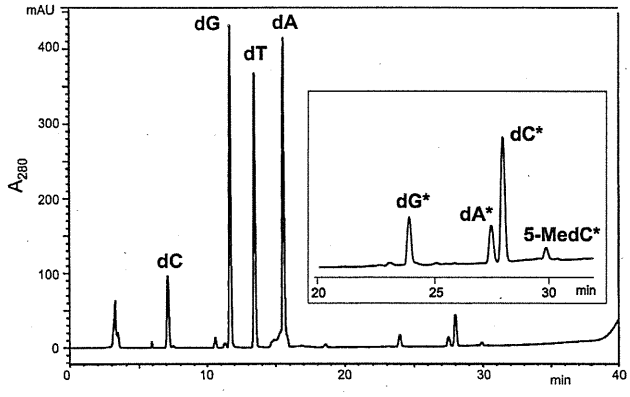

Figure 5. Analysis of 4-OHE−DNA adducts formed in vitro by HPLC. Inset, the chromatogram (20−32 min) was expanded. Column: Inertsil ODS-3, 3 μm, 4.6 mm × 250 mm (GL Sciences Inc., Japan); elution: 0−40 min, linear gradient of acetonitrile (5−30%); elution speed: 0.7 mL/min.

Table 4. Adduct Levels in 4-OHE-Treated Calf Thymus DNA in Vitro

	dC*	dA*	dG*	5-Me-dC*
adduct/10^3 each parent base	41.5/10^3 dC	6.38/10^3 dA	5.58/10^3 dG	61.5/10^3 5-Me-dC
μg adduct/100 μg DNA	0.88	0.18	0.12	0.08

LC/MS/MS Analysis of 4-OHE Adducts in Organ DNA from 4-OHE-Treated Mice. The 4-OHE−DNA adducts in vivo were detected by an LC/MS/MS method. Figure 6 shows typical ion chromatograms of dG*, dA*, 5-Me-dC*, and dC* in DNA isolated from the stomachs of control- and 4-OHE-treated mice. Quantification of the 4-OHE−DNA adducts was achieved using $[^{15}N_5]$-dA* and $[^{15}N_3]$-dC* as internal standards. Some uncertainty remained in the analyses of dG* and 5-Me-dC*, since isotopically labeled dG* and 5-Me-dC* were not used. The results of the DNA adduct formation in mouse stomach and large intestine at 24 h after the oral administration of 4-OHE are summarized in Table 5. Only background levels of the adducts were present in the organ DNA of the vehicle-treated, control mice. In the stomach and large intestine DNA of 4-OHE-treated mice, dC* was detected in the range of 43.71 and 5.57 adducts per 10^8 bases, respectively. dA* was detected at a comparable level to dC* in these organs. In addition, lower amounts of dG* and 5-Me-dC* were detected in these organ DNAs. The amounts of these DNA adducts were decreased at 72 h after administration (Table 5), and no DNA adduct was detected after 7 days in these organ DNAs (data not shown). Additionally, with intragastric administration, no 4-OHE−DNA adducts were detected in the liver and kidney DNA (data not shown). In separate, independent mice experiments with the same 4-OHE dose, dC*, dG*, and 5-Me-dC* were also detected in the esophagus DNA in the range of 5.1 ± 5.9, 2.7 ± 0.7, and 1.0 ± 1.2 adducts per 10^8 bases ($n = 3-4$), respectively.

4-OHE Adduct Analysis in Human Lung DNA. An LC/MS/MS method was used to detect 4-OHE adducts in human lung DNA (Figure 7). dC* was detected in all lung tissues, in the range of 2.6−5.9/10^9 bases, while dA* was detected in three samples (Table 6). dG* and 5-Me-dC* were not detected. The mean dC* and dA* levels in DNA were 4.04 and 1.75/10^9 bases, respectively. The levels of dC* and dA* did not significantly correlate with cigarette smoking or aging. These results suggested that 4-OHE−DNA adducts are commonly present in human lung tissue and may be useful as endogenous biomarkers of oxidative stress. However, to establish its presence in human lung tissue unambiguously, the peak attributed to dC* in the chromatogram should be confirmed by monitoring a second product ion and carefully confirming the retention times and the relative peak heights of the two products ions, as compared to a dC* standard.

Discussion

This is the first report of the in vivo detection and quantification of 4-OHE−DNA adducts using an LC/MS/MS method. As described in the introduction, 4-OHE is mutagenic and is commonly present in our food, as a lipid oxidation product. Because dietary habits are a major factor in human carcinogenesis (*18*), the relation between the intake of 4-OHE via food

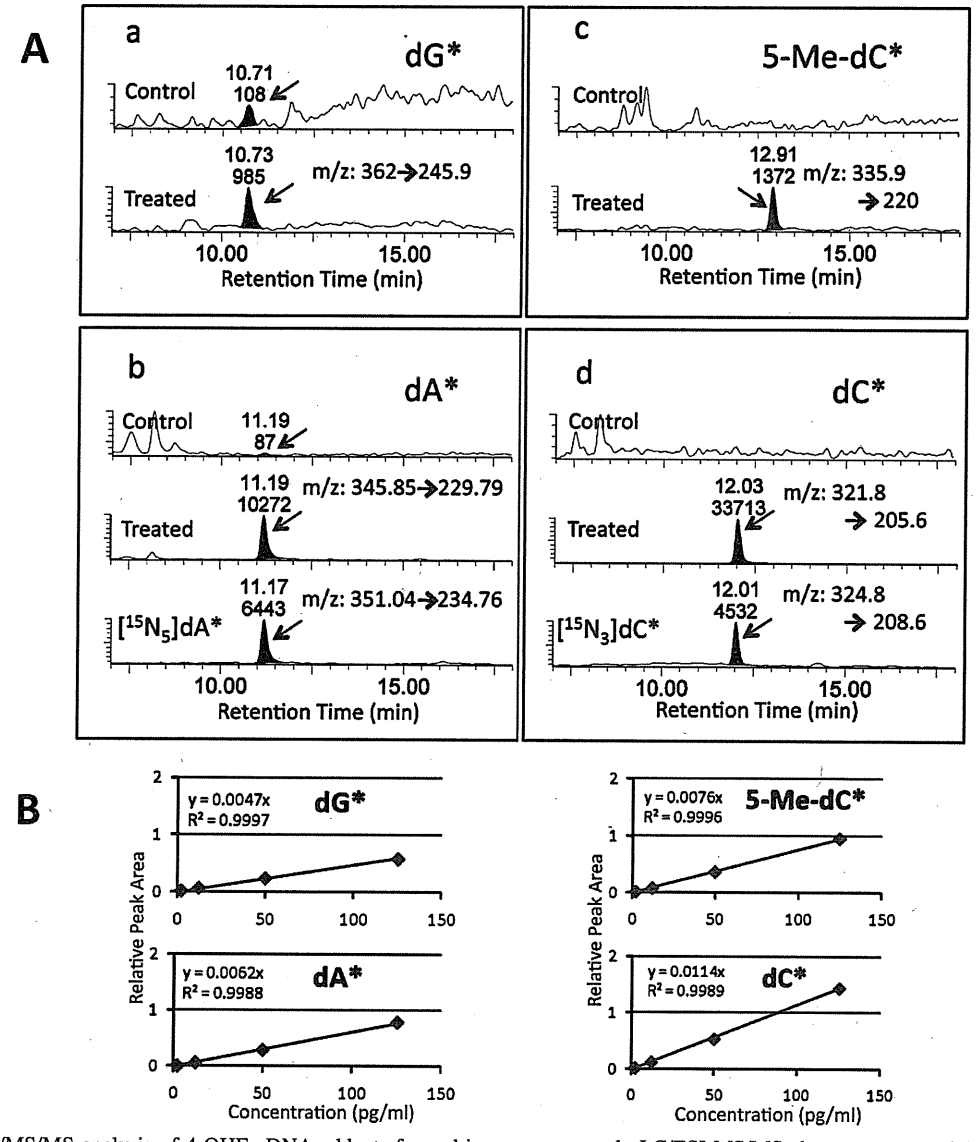

Figure 6. (A) LC/MS/MS analysis of 4-OHE−DNA adducts formed in mouse stomach. LC/ESI-MS/MS chromatograms of 4-OHE adducts and internal standards detected in mouse stomach DNA isolated from control- and 4-OHE-treated mice. Retention time (upper) and peak area (lower) are shown above each peak. (a) dG*, (b) dA*, (c) 5-Me-dC*, and (d) dC*. (B) Calibration curves for dG*, dA*, 5-Me-dC*, and dC*.

and carcinogenicity must be examined. So far, long-term carcinogenicity studies on 4-OHE have not been reported; however, as described in the Results, 4-OHE, like other carcinogenic α,β-unsaturated carbonyl compounds, such as acrolein or crotonaldehyde, forms DNA adducts in vivo.

The oral administration route of 4-OHE in mice resulted in DNA adduct formation in the digestive tract, for example, esophagus, stomach, and large intestine, but not in liver and kidney. It seems that the 4-OHE was directly absorbed after the i.g. administration by the esophageal, stomach, and large intestine tissues but was not distributed into the liver. The adduct distribution in the organs demonstrates a tendency of formation at the site of first contact with 4-OHE. The adduct levels decreased continuously during 7 days after administration (data not shown). The 4-OHE−DNA adducts might be repaired to a certain extent; however, the decrease in the adduct level can also be explained, at least in part, by cell turnover.

The formation of 4-hydroxy-2-nonenal and 4-oxo-2-nonenal (4-ONE) by ω-6 lipid peroxidation in biological systems and their adduct formation with proteins and DNA have been well-studied,

Table 5. Levels of 4-OHE−DNA Adducts in Mouse Organs[a]

				adducts/10^8 bases			
		mg/mouse	h after treatment	dC*	dA*	dG*	5-Me-dC*
stomach	control	0	24	ND	0.3 ± 0.7	0.2 ± 0.3	ND
	4-OHE	3	24	43.7 ± 24.7	30.2 ± 33.2	5.5 ± 3.2	3.4 ± 5.5
	4-OHE	3	72	2.3 ± 2.6		0.6 ± 0.6	ND
large intestine	control	0	24	ND	0.2 ± 0.4	0.1 ± 0.3	ND
	4-OHE	3	24	5.6 ± 6.5	3.0 ± 3.4	1.0 ± 1.2	0.3 ± 0.7
	4-OHE	3	72	0.5 ± 1.2		0.2 ± 0.3	ND

[a] Data represent the mean ± SD; $n = 6-8$.

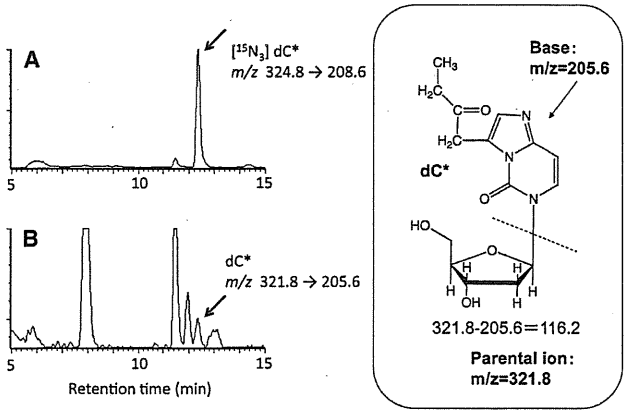

Figure 7. LC/MS/MS analysis of 4-OHE–DNA adducts in human lung DNA. (A) Analysis of ^{15}N-dC*. The transition *m/z* 324.8→208.6 was monitored. (B) Analysis of dC*. The transition *m/z* 321.8→205.6 was monitored. A smoothing method was employed to improve the S/N value.

Table 6. Levels of 4-OHE–DNA Adducts in Human Lung DNA[a]

				adducts/10^9 bases	
patient	sex	age	smoking (BI)	dC*	dA*
1	male	52	1280	3.6	ND
2	male	65	585	4.9	4.6
3	male	77	1500	3.7	ND
4	male	79	1160	5.9	3.9
5	female	56	0	3.3	ND
6	female	65	0	3.8	ND
7	female	70	0	4.4	ND
8	female	70	25	2.6	9.0
9	female	71	0	4.7	ND
10	female	76	0	3.5	ND

[a] dG* and 5-Me-dC* were not detected. BI, Brinkman index.

as markers of endogenous oxidative stress in relation to lipid peroxidation (*4, 22*). For example, 4-hydroxy-2-nonenal–protein adducts have been found in the lung tissues from patients with chronic pulmonary disease (*23*). Blair and his collaborators detected a 4-ONE adduct with glutathione and suggested that it is a good marker of cellular oxidative stress (*24*). Our discovery of 4-OHE has two important implications: (1) It may be a food mutagen produced during cooking or storage; for example, fried fish and old cooking oil contain large amounts of 4-OHE; and (2) it may also be an endogenous mutagen produced by lipid peroxidation in membranes in vivo. Protein-bound forms of an ω-3 lipid peroxidation product, 4-hydroxy-2-hexenal, were detected in the liver tissues from patients with chronic hepatitis C (*25*). In the present study, we detected dC* clearly in all of the human lung DNA samples. Therefore, 4-OHE–DNA adducts may be useful markers of environmental exposure to 4-OHE and endogenous oxidative stress in relation to cancer induction.

Acknowledgment. This work was supported by grants from the Ministry of Health, Labor and Welfare of Japan.

Supporting Information Available: ^{1}H–^{13}C HMBC spectrum of 5-Me-dC*, ^{1}H–^{15}N HMBC spectrum of 5-Me-dC*, ^{1}H–^{15}N HMBC spectrum of dA*, and mass spectra of dC*, 5-Me-dC*, and dA* obtained by HRESI-MS/MS analyses. This material is available free of charge via the Internet at http://pubs.acs.org.

References

(1) Esterbauer, H. (1993) Cytotoxicity and genotoxicity of lipid-oxidation products. *Am. J. Clin. Nutr. 57*, S779–S786.

(2) Esterbauer, H., Schaur, R. J., and Zollner, H. (1991) Chemistry and biochemistry of 4-hydroxynonenal, malonaldehyde and related aldehydes. *Free Radical Biol. Med. 11*, 81–128.

(3) Chung, F. L., Young, R., and Hecht, S. S. (1984) Formation of cyclic adducts of 1,N^2propanodeoxyguanosine adducts in DNA upon reaction with acrolein or crotonaldehyde. *Cancer Res. 44*, 990–995.

(4) Blair, I. A. (2001) Lipid hydroperoxide-mediated DNA damage. *Exp. Gerontol. 36*, 1473–1481.

(5) Cajelli, E., Ferraris, A., and Brambilla, G. (1987) Mutagenicity of 4-hydroxynonenal in V79 Chinese hamster cells. *Mutat. Res. 190*, 169–171.

(6) Marnett, L. J., Hurd, H. K., Hollstein, M. C., Levin, D. E., Esterbauer, H., and Ames, B. N. (1985) Naturally occurring carbonyl compounds are mutagens in Salmonella tester strain TA104. *Mutat. Res. 148*, 25–34.

(7) Shields, P. G., Xu, G. X., Blot, W. J., Fraumeni, J. F., Trivers, G. E., Pellizzari, E. D., Qu, Y. H., Gao, Y. T., and Harris, C. C. (1995) Mutagens from heated Chinese and U.S. cooking oils. *J. Natl. Cancer Inst. 87*, 836–841.

(8) Fujioka, K., and Shibamoto, T. (2006) Determination of toxic carbonyl compounds in cigarette smoke. *Environ. Toxicol. 21*, 47–54.

(9) Burcham, P. C. (1999) Internal hazards: Baseline DNA damage by endogenous products of normal metabolism. *Mutat. Res., Genet. Toxicol. Environ. Mutagen. 443*, 11–36.

(10) Kasai, H., Maekawa, M., Kawai, K., Hachisuka, K., Takahashi, Y., Nakamura, H., Sawa, R., Matsui, S., and Matsuda, T. (2005) 4-oxo-2-hexenal, a mutagen formed by omega-3 fat peroxidation, causes DNA adduct formation in mouse organs. *Ind. Health 43*, 699–701: ibid; 46, 101, 2008.

(11) Maekawa, M., Kawai, K., Takahashi, Y., Nakamura, H., Watanabe, T., Sawa, R., Hachisuka, K., and Kasai, H. (2006) Identification of 4-oxo-2-hexenal and other direct mutagens formed in model lipid peroxidation reactions as dGuo adducts. *Chem. Res. Toxicol. 19*, 130–138.

(12) Kawai, K., Matsuno, K., and Kasai, H. (2006) Detection of 4-oxo-2-hexenal, a novel mutagenic product of lipid peroxidation, in human diet and cooking vapor. *Mutat. Res. 603*, 186–192.

(13) Kasai, H., and Kawai, K. (2008) 4-oxo-2-hexenal, a mutagen formed by omega-3 fat peroxidation: Occurrence, detection and adduct formation. *Mutat. Res., Rev. Mutat. Res. 659*, 56–59.

(14) Rindgen, D., Nakajima, M., Wehrli, S., Xu, K. Y., and Blair, I. A. (1999) Covalent modifications to 2′-deoxyguanosine by 4-oxo-2-nonenal, a novel product of lipid peroxidation. *Chem. Res. Toxicol. 12*, 1195–1204.

(15) Lee, S. H., Rindgen, D., Bible, R. H., Hajdu, E., and Blair, I. A. (2000) Characterization of 2′-deoxyadenosine adducts derived from 4-oxo-2-nonenal, a novel product of lipid peroxidation. *Chem. Res. Toxicol. 13*, 565–574.

(16) Pollack, M., Oe, T., Lee, S. H., Elipe, M. V. S., Arison, B. H., and Blair, I. A. (2003) Characterization of 2′-deoxycytidine adducts derived from 4-oxo-2-nonenal, a novel lipid peroxidation product. *Chem. Res. Toxicol. 16*, 893–900.

(17) Kawai, Y., Uchida, K., and Osawa, T. (2004) 2′-Deoxycytidine in free nucleosides and double-stranded DNA, as the major target of lipid peroxidation products. *Free Radical Biol. Med. 36*, 529–541.

(18) Sugimura, T. (2002) Food and cancer. *Toxicology 181*, 17–21.

(19) Wang, T. J., Zhou, B. S., and Shi, J. P. (1996) Lung cancer in nonsmoking Chinese women: A case-control study. *Lung Cancer 14*, S93–S98.

(20) Zhong, L. J., Goldberg, M. S., Gao, Y. T., and Jin, F. (1999) Lung cancer and indoor air pollution arising from Chinese style cooking among nonsmoking women living in Shanghai, China. *Epidemiology 10*, 488–494.

(21) Matsuda, T., Yabushita, H., Kanaly, R. A., Shibutani, S., and Yokoyama, A. (2006) Increased DNA damage in ALDH2-deficient alcoholics. *Chem. Res. Toxicol. 19*, 1374–1378.

(22) Douki, T., Odin, F., Caillat, S., Favier, A., and Cadet, J. (2004) Predominance of the 1, N^2propano 2′-deoxyguanosine adduct among 4-hydroxy-2-nonenal-induced DNA lesions. *Free Radical Biol. Med. 37*, 62–70.

(23) Rahman, I., van Schadewijk, A. A. M., Crowther, A. J. L., Hiemstra, P. S., Stolk, J., MacNee, W., and De Boer, W. I. (2002) 4-Hydroxy-2-nonenal, a specific lipid peroxidation product, is elevated in lungs of patients with chronic obstructive pulmonary disease. *Am. J. Respir. Crit. Care Med. 166*, 490–495.

(24) Blair, I. A. (2006) Endogenous glutathione adducts. *Curr. Drug Metab. 7*, 853–872.

(25) Kitase, A., Hino, K., Furutani, T., Okuda, M., Gondo, T., Hidaka, I., Hara, Y., Yamaguchi, Y., and Okita, K. (2005) In situ detection of oxidized n-3 polyunsaturated fatty acids in chronic hepatitis C: Correlation with hepatic steatosis. *J. Gastroenterol. 40*, 617–624.

TX9003819

COMMENTARY

液体クロマトグラフィータンデム質量分析法を用いたDNA損傷研究法

Quantification of DNA Adducts by Using Liquid Chromatography/Tandem Mass Spectrometry

松田知成[1]*・永吉晴奈[2]・椙村春彦[3]・周　佩欣[4]
Tomonari MATSUDA,[1]* Haruna NAGAYOSHI,[2]
Haruhiko SUGIMURA,[3] and Pei-Hsin CHOU[4]

[1] 京都大学大学院工学研究科附属流域圏総合環境質研究センター　*Research Center for Environmental Quality Management, Kyoto University, Otsu, SHIGA, JAPAN*
[2] 大阪府公衆衛生研究所　*Osaka Prefectural Institute of Public Health, Osaka, JAPAN*
[3] 浜松医科大学　*Hamamatsu University School of Medicine, Hamamatsu, JAPAN*
[4] 国立成功大学　*National Cheng Kung University, Tainan, TAIWAN*

Formation of DNA adducts is a crucial step for carcinogenesis and aging. However, until recently, it was difficult to quantify trace amount of DNA adducts in living organisms. Development of liquid chromatography/tandem mass spectrometry (LC/MS/MS) equipments enables us to quantify DNA adducts at practical sensitivity. Molecular epidemiological study such as aldehyde dehydrogenase 2 gene (*ALDH2*) genotypes and risk of alcohol-related DNA damage has been conducted by using LC/MS/MS. Furthermore, we developed "DNA adductome" analysis which can display comprehensive picture of DNA adducts in living organisms. These techniques may contribute to understand mechanisms of carcinogenesis and aging.

(Received April 27, 2009; Accepted June 8, 2009)

1. DNA付加体とは

DNA付加体とは，外来の発がん物質や生体内で生じる反応性に富む化学種が，DNAと共有結合したものである．DNAはアデニン，グアニン，チミン，シトシン，および5メチルシトシンの5種類の塩基，デオキシリボース，そしてリン酸からなる高分子である．化学物質はこのうちどの部分も攻撃しうるが，塩基部分への付加体について特によく研究されている．本稿においてはDNA塩基部分への付加体の意味で，「DNA付加体」という言葉を使用する．

ある種のDNA付加体は，細胞分裂の際DNA合成を阻害し，細胞死や突然変異を誘発する．この結果，DNA付加体は突然変異，発がん，加齢に密接に関連すると考えられている．数多くのDNA付加体についてその突然変異への寄与，DNA修復されやすさなどが調べられているものの，DNA付加体の種類は多種多様であり，生体内の付加体について全容が明らかになっているわけではない．

2. DNA付加体のさまざまな測定法

生体に対するDNA付加体の影響を調べるため，付加体の検出が試みられてきたが，微量なDNA付加体を検出・定量することは，最近まで非常に困難であった．^{32}P-ポストラベル法はDNA付加体の分析に最もよく使われてきた方法である．ヌクレアーゼP1法やブタノール抽出法，非変性poly-acrylamide gel electrophoresis (PAGE) 分離法などの変法も開発され，分子量の大きな化合物の付加体（例えば代表的な発がん物質ベンゾ[*a*]ピレンの付加体など）については非常に感度よく定量できる[1]．しかし，低分子量の付加体（例えば水酸基やメチル基が付いただけのものなど）をこの方法で解析することは極めて困難であった．

ガスクロマトグラフ質量分析計や液体クロマトグラフ質量分析計を使う方法も有望である．これらの分析機器を用いれば，数種類のDNA付加体を同時に定量的に測定できる．ガスクロマトグラフを用いる場合はDNAを加水分解

本稿は第35回BMSコンファレンスでの講演内容を著したものです．

* Correspondence to: Tomonari MATSUDA, *Research Center for Environmental Quality Management, Kyoto University, 1-2 Yumihama, Otsu, Shiga 520-0811, JAPAN*, e-mail: matsuda@z05.mbox.media.kyoto-u.ac.jp
松田知成，京都大学大学院工学研究科附属流域圏総合環境質研究センター，〒520-0811 大津市由美浜1-2

して塩基部分を測定する．一方，液体クロマトグラフは，酵素でデオキシヌクレオシドに分解して測定するのが一般的である．これらの中で液体クロマトグラフィータンデム質量分析法 (liquid chromatography/tandem mass spectrometry: LC/MS/MS) は，デオキシヌクレオシドを最も感度よく測定できる機器である．LC/MS/MS を用いて DNA 付加体を測定する試みは今までにいくつかあったが，一世代前の LC/MS/MS を用いたこれらの研究では，少量の DNA サンプルから DNA 付加体を測定するには感度が不十分であった．しかし最新型の LC/MS/MS を用いれば，5 μg の DNA からでも 10^8 塩基当たり数個の DNA 付加体が定量可能で，検出だけなら，10^9 塩基当たり数個のレベルまで到達していることを筆者は確認した[2]．これは，^{32}P-ポストラベル法に迫る感度である．また，LC/MS/MS の分析では 10 種類以上のイオンの質量を，感度を落とすことなく同時にモニターでき，複数の DNA 付加体を同時に定量可能であるという利点もある．簡便性，定量性，再現性では LC/MS/MS は ^{32}P-ポストラベル法を凌駕している．DNA 付加体の分析法は早晩 LC/MS/MS が主流になるだろう．

3. LC/MS/MS による DNA 付加体の分析法

まず，臓器や培養細胞などの生体サンプルから DNA を抽出する．きれいに精製できればどのような方法でも良いと思うが，測定する付加体の種類によっては特別な精製法が必要である．例えば，酸化的 DNA 損傷 8-oxo-dG を測定する際は DNA 抽出の過程で自然に生成しやすいので，DNA 抽出に使用する緩衝液に酸化を抑制する試薬を加える．また，後述するアセトアルデヒドの DNA 付加体を測定する際には，DNA 抽出過程でエタノール沈殿の代わりにイソプロパノール沈殿を行ったりする（エタノールに不純物としてアセトアルデヒドが含まれるため）．

DNA が精製できたら次は DNA を酵素で分解し，デオキシヌクレオシド体にする．これもいくつかの方法があるが，われわれは Micrococcus Nuclease, Spleen phosphodiesterase II, およびアルカリフォスファターゼという 3 種類の酵素を用いている．

次はいよいよ LC/MS/MS の測定である．Fig. 1 に例として N^2-ethyl-dG という DNA 付加体の開裂パターンを示す．付加体デオキシヌクレオシドの多くはエレクトロスプレーイオン化法により，プロトンが 1 個付加した正イオン（プロトン付加分子）を生じる．このイオンが衝突セルに導入されると，多くの場合，デオキシリボースと塩基間のグリコシド結合が開裂し，塩基部分の質量＋1 のプロダクト（フラグメント）イオンを生じる．デオキシリボース部分の質量は 116 なので，塩基部分の質量は必ずデオキシヌクレオシドの質量－116 になる．したがって，デオキシヌクレオシドの質量を M としたとき，プリカーサーイオンを M＋1，プロダクトイオンを (M－116)＋1 に設定して，multiple reaction monitoring (MRM) スキャンを行うと，ほとんどの場合うまく DNA 付加体を測定することができる．

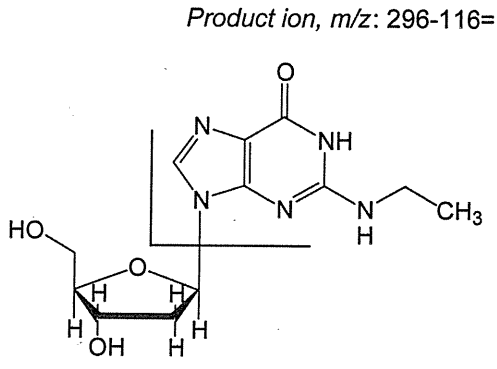

Fig. 1. Degradation pattern of DNA adducts in LC/MS/MS analysis. This figure shows the structure of N^2-ethyl-dG as an example of DNA adducts. In many cases, the glycoside bond, which links deoxyribose and DNA base, is easily broken in CID (collision-induced dissociation) cell.

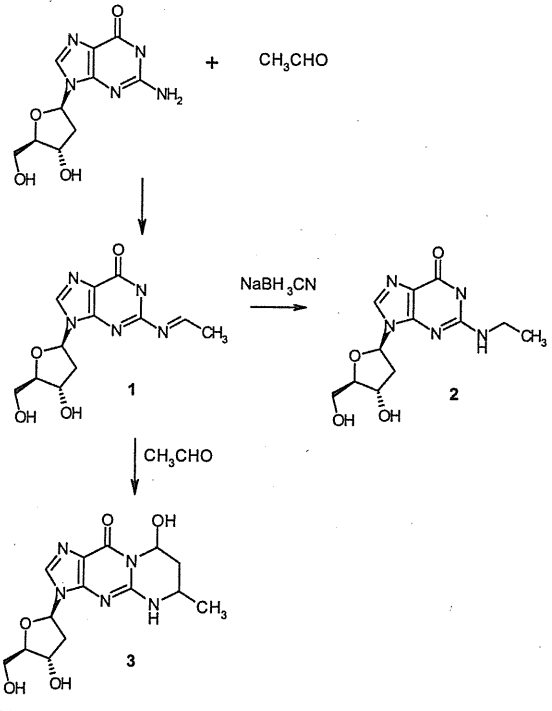

Fig. 2. Formation of acetaldehyde-dG adducts. 1: N^2-ethylidene-dG, 2: N^2-ethyl-dG, 3: α-Me-γ- OH-PdG

4. DNA 付加体の測定例

筆者らはこのような方法でさまざまな DNA 付加体の定量を行っているが，次にその一例を示したい．読者の中にはお酒が好きな人も多いと思うが，お酒を飲むとすぐ赤くなる人（専門用語でフラッシャーという）は，飲酒による食道がんのリスクが非常に高くなる[3]．エタノールは体内で酸化されて反応性の高いアセトアルデヒドになる．アセトアルデヒドはアルデヒド脱水素酵素 (aldehyde dehydrogenase 2: ALDH2) によって酢酸へと無毒化されるが，